Mapping of Urban Heat Hotspots in Delhi, Rajkot and Bhubaneswar

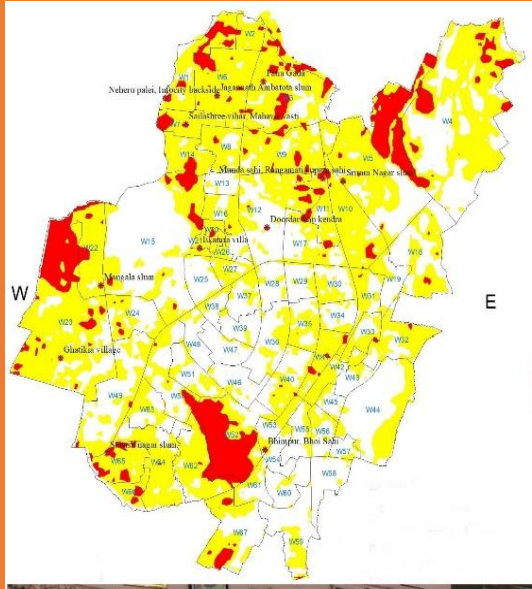

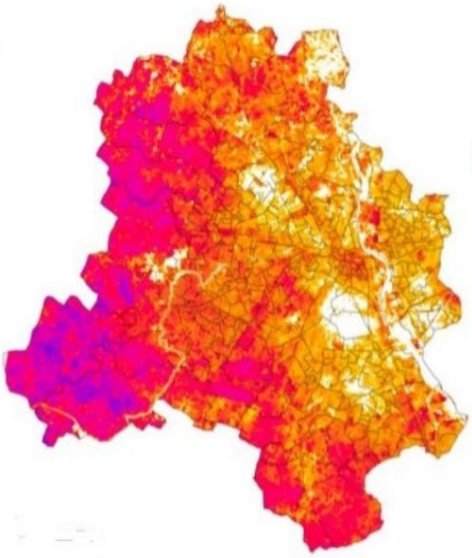

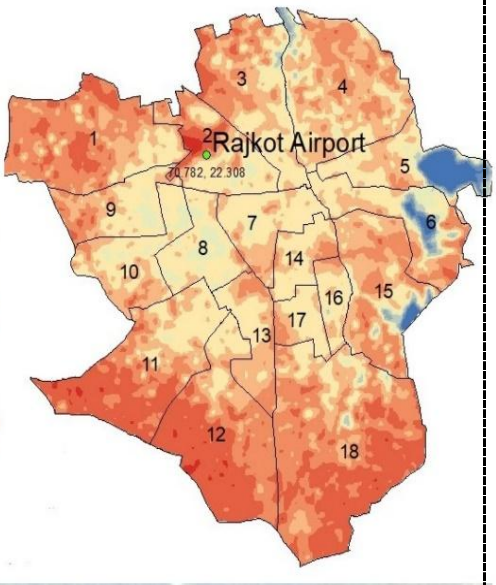

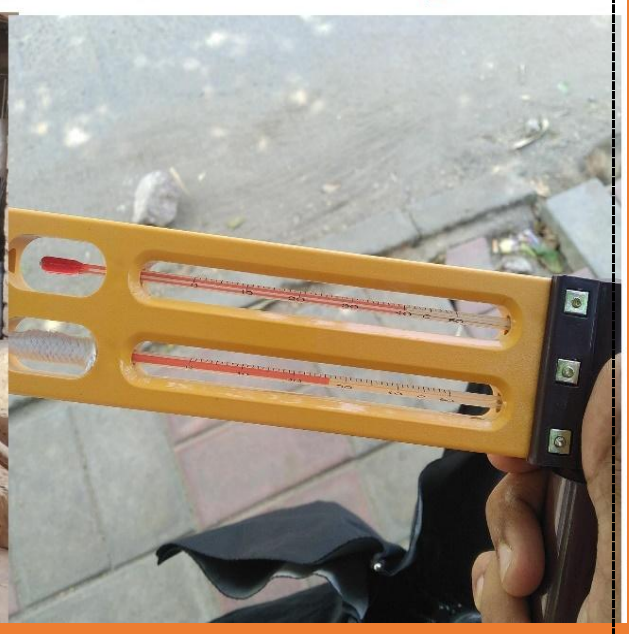

Integrated Research and Action for Development (2019)

IDRC | CRDI Canada
15 Integrated Research and IRADe Action for Development

Citation: Magotra, R., Kumar, M., Bhatia, A., & Tyagi, A. (2019). Mapping of urban heat hotspots in Delhi, Rajkot and Bhubaneswar, 2019.

Integrated Research and Action for Development

C-80, Shivalik Colony, Malviya Nagar,
New Delhi, 110017, India
Tel: 91 (11) 2667 6180, 2667 6181, 40667781
Email: info@irade.org

Website: http://www.irade.org

Table of Contents

1. Introduction 1
2. Study Area 4
3. Methodology 6
4. Results and Discussions 9
5. Conclusion 29
6. References: 29
7. Acknowledgements iv

List of Figures

Figure 1: Mortality due to heat stroke in Delhi during 2001-14 2

Figure 2: Location of three Indian cities studied in the project 4

Figure 3: Flowchart depicting calculation of LST from satellite image 9

Figure 4: LST map of Delhi for 30 May 2019 11

Figure 5: Spatial variation of maximum ambient air temperature on 30 May 2019 as per the data recorded by DPCC monitors 11

Figure 6: LST maps of Delhi for 27 May 2018 and 12 June 2018 12

Figure 7: Map showing hotspots above 40° C in Delhi on 6 April 2017 13

Figure 8: LST distribution in Rajkot on, 04 May and 14 June,2017 14

Figure 9: LST distribution in Rajkot on, 07 May and 08 June, 2018 15

Figure 10: Map showing AWS and slum locations in Rajkot 16

Figure 11: Survey locations in Rajkot 16

Figure 12: Thermal hotspots in Rajkot with LST =/> 42 °C 17

Figure 13: LST and hotspot maps for Bhubaneswar for 12 April 2017 (above) and 14 May 2017 (below) 18

Figure 14: Maps showing dry-bulb air temperature (a), wet-bulb temperature (b) and RH (c) measured in Bhubaneswar on 09 May 2018 21

Figure 15: Dry bulb air temperature recorded in Bhubaneswar at 10:30 AM and 2:30 PM on 10 March 2019 22

Figure 16: Map showing wet-bulb air temperature measured at several locations in Bhubaneswar on 10 March 2019 at 10:30 AM and 2:30 PM 23

Figure 17: Maps showing RH at surveyed locations in Bhubaneswar as on 10 March 2019 at 10:30 AM and 2:30 PM 24

Figure 18: Dry bulb air temperature recorded in Bhubaneswar at 10:30 AM and 2:30 PM on 26 March 2019 25

Figure 19: Map showing wet-bulb air temperature measured at surveyed locations in Bhubaneswar on 26 March 2019 at 10:30 AM and 2:30 PM 26

Figure 20: Maps showing RH at surveyed locations in Bhubaneswar as on 26 March 2019 at 10:30 AM and 2:30 PM 27

Figure 21: Map showing LST of Bhubaneswar as on 10 March 2019. The LST of surveyed locations has been highlighted separately. 28

Figure 22: Map showing LST of Bhubaneswar as on 26 March 2019. The LST of surveyed locations has been highlighted separately. 28

List of Tables

Table 1: Comparative Assessment of Satellite Data Available for Thermal Mapping 6

Table 2: Thermal hot-spots surveyed in Delhi based on LST maps 13

Table 3: Thermal hotspots surveyed in Bhubaneswar 19

Acknowledgements

We sincerely acknowledge the support and cooperation received from the International Development Research Centre (IDRC), the India Meteorological Department (IMD), the Delhi Pollution Control Committee (DPCC), and the Regional Meteorological Centre (RMC) for their valuable guidance, institutional support, and provision of essential data and resources that significantly contributed to the successful completion of this research work.

The authors also express their gratitude to all experts, officials, and stakeholders who directly or indirectly supported this research.

Rohit Magotra

Principal Investigator, IRADe

1. Introduction

There has been unprecedented growth of urban areas across the world in the past few decades. For example, in 2018, the global urban population was around 55% of the total population of the world; and this figure is set to increase to nearly 68% by 2050 (UN, 2018). Increased urbanisation has modified many biophysical processes influencing energy balance, infiltration, storm-water runoff, precipitation, temperature, air quality, carbon storage and local biodiversity of an area (dos Santos et al., 2017). One of the alarming concerns of urbanization is rapid increase of local ambient temperature (both air temperature as well as land surface temperature), which significantly impacts the life of urban citizens. The increase in temperature within the urban centers, relative to surrounding rural areas, gives rise to what is popularly known as Urban Heat Island (UHI). The intra-city urban heat islands form when the land cover dominated by natural vegetation, agricultural crops and water bodies, is replaced by heat-absorbing impervious surfaces composed of materials like concrete and asphalt (Simwanda et al., 2019; Buyantuyev and Wu, 2010). These UHIs make daily livelihood activities difficult for human beings as our optimum physiological range of temperature for proper functioning, is exceeded. Many of these human health impacts of elevated temperatures are manifested in the form of cardiovascular, cerebrovascular and respiratory ailments (Sharma et al., 2019). These urban heat islands occurring continuously over the same area for few days create heat waves.

The UHI incidents, and in turn the incidences of heat waves, have increased in recent years, due to climate change. As predicted by IPCC (Intergovernmental Panel on Climate Change), the incidences of heat waves are supposed to increase in future even under RCP 4.5 scenario (IPCC, 2013; Sharma et al., 2019). IPCC report also suggest an increase in the frequency and duration of the heat waves in near future (IPCC, 2013; Sharma et al., 2019).

Over a period of 1990-2009, the mean annual temperature across India increased by 1°C relative to that during the period 1961-1990 (Sharma et al., 2019; Attri and Tyagi, 2010). In particular, during the summer months of March-May, the country faces heat waves in one or more areas almost every year (Mishra et al., 2017; Rohini et al., 2016; Pai et al., 2013). Eleven of India's 15 warmest years have occurred since 2004, and 2018 was the sixth-warmest year for the country since record-keeping started in 1901 (NASA Earth Observatory, 2019). The increased events of heat stress over the years has caused many fatal incidents in India. For instance, in 1998 and 2015, parts of India experienced heatwaves that resulted in more than 2000 deaths each (EM-DAT,

2019; Mishra et al., 2017). The deaths occurring in Delhi due to heat stroke during 2001-14 are shown in Figure 1.

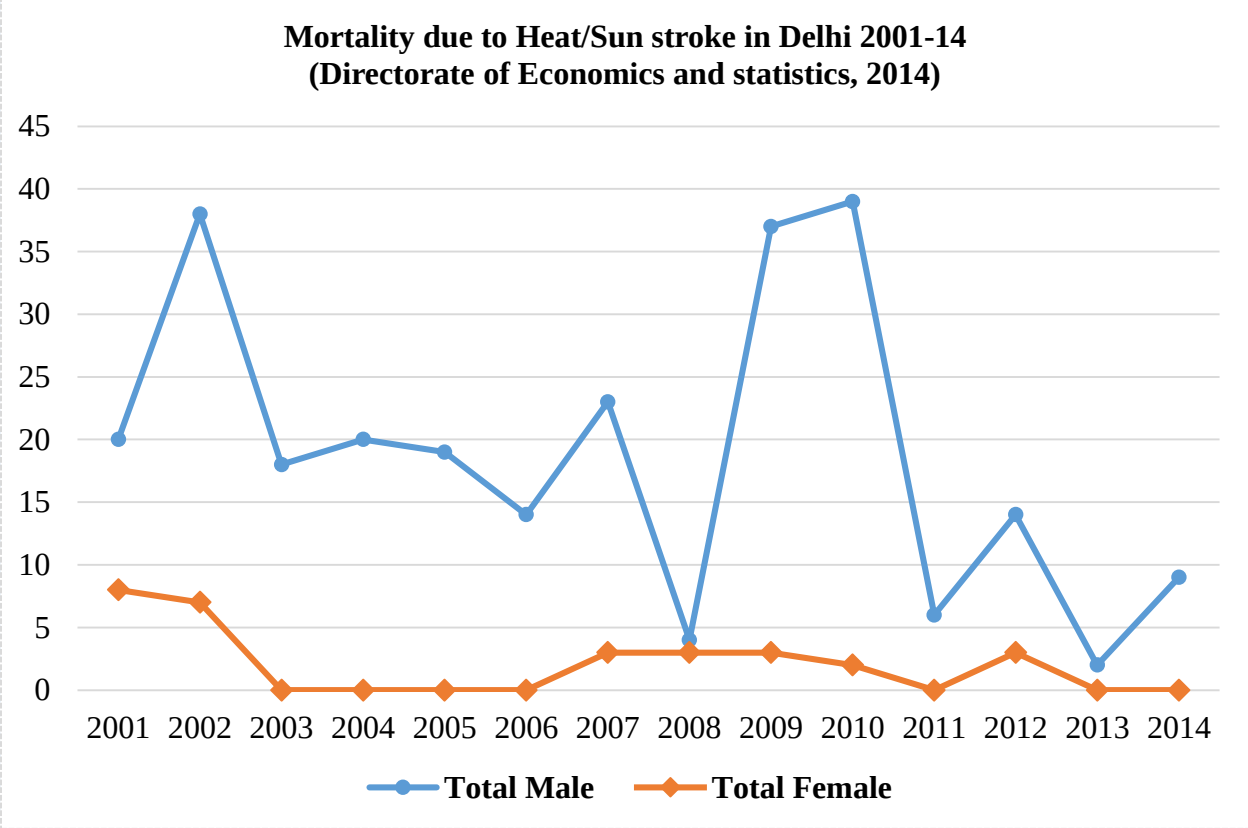

Figure 1: *Mortality due to heat stroke in Delhi during 2001-14*

It is therefore important to map and monitor the Land Surface Temperature as well as Ambient Air Temperature because the warmth absorbed by the ground and air creates heat islands and hotspots, which affect the *in situ* micro climate of a place as well as *ex situ* climate at a major regional scale.

The thermal hot-spot maps give insight in the differences in hot spot distribution within the cities. Identifying hot spots within a city can help focus interventions where they are most needed during heat waves. We consider 'hot-spots' as the areas within the city which experience ambient temperature in excess of the average monthly maximum temperature of the city. Such thermal maps provide information about the areas which have the accumulation of hotspots, and therefore population living there is under high physiological and socio-economic risks due to thermal stress. Thus, specific measures to curb the problem of heat stress for the

resident population can be taken using these maps. In addition, a comparative study of thermal hot-spot maps for each season will help to identify the months in which most cautions need to be taken.

For ambient air temperature, we mostly rely on measurements provided by meteorological stations, or taken by the researchers using hand-held portable devices. However, these measurements are mostly taken at a point and may not sufficiently represent the temperature of entire locality. Satellite remote sensing provides an attractive alternative as the satellites cover a large swath of earth's surface. In particular, the land surface temperature measured by satellites in thermal infrared region of electromagnetic spectrum has been used by various researchers across the globe (Zhang and Cheng, 2019; Wang et al., 2017; Jin, 2012; Zhang and Kainz, 2012; Yuan and Bauer, 2007; Chen et al., 2006) , and in some instances, these satellite-derived land surface temperatures have been correlated with ambient air temperatures to obtain a complete picture of the study area (Mutiibwa et al., 2015; Unger, 2009; Vadasz, 1994).

Between 2017-2019, IRADe undertook a study to assess and describe spatial distributions of human vulnerability to extreme heat events and provide evidences and recommendations to develop adaption measures and information to target emergency responses during heat wave events. Our study areas were three Indian cities: Delhi, Rajkot and Bhubaneswar. The study identified professions that require enduring heat such as mobile workers (drivers of auto-rickshaws, scooters, taxis), stationary workers such as traffic police, small shop-keepers and footpath vendors, construction workers and their families that stay in make shift shelters, slum dwellers, domestic women workers, women vendors.; children, pregnant women and suggested adaptation strategies for coping with extreme heat wave events.

As a part of the study, we used thermal images from Landsat-8 satellite to map the Land Surface Temperature of the three project cities, and then identified the hot-spots. In addition, data on ambient air temperature measured by Automatic Weather Stations (AWS) was procured from IMD (India Meteorological Department) and municipal corporations, and mapped. This report provides in detail the procedure of temperature mapping and the results obtained. The findings provide city administrators and policymakers with spatially explicit evidence to prioritise heat stress interventions and inform Heat Stress Action Plans.

2. Study Area

The study was carried out in three Indian cities, *viz.*, Delhi, Rajkot and Bhubaneswar (Figure 2).

Figure 2: *Location of three Indian cities studied in the project*

2.1. Delhi:

Delhi, the capital city of India, is situated in the central part of the country. The city is located between 28°24'17"N and 28°53'00"N latitude, and 76°50'24" E and 76°20'37"E longitude. It has an area of approx. 1483 sq. km. and a population of around 16 million (census of India, 2011). It is a completely landlocked city, which experiences extremes of both summer and winter seasons. During winters, the temperature drops to nearly 2 °C under the influence of chilling winds coming from the Himalaya in the north. On the other hand, summers experience extreme heat waves due to hot winds blowing from the Thar Desert in the west. The summer season lasts from March to June, whereas winters start late in October and extend to the end of February. Monsoon season is sandwiched in the middle, from July to September. The city's urban area of influence, called "National Capital Region (NCR)", is considered beyond its boundaries of National Capital

Territory (NCT), and encompasses the satellite cities like Gurgaon, Faridabad, Ghaziabad etc. Due to high population density, the inhabitants are highly vulnerable to the adverse impacts of extreme heat stress. The deaths occurring in Delhi due to heat stroke during 2001-14 are shown in Figure 1. Relatively higher deaths of males is apparently attributable to their outdoor working lifestyle.

2.2. Rajkot:

Rajkot is situated in the western part of the country, and is characterised by a semi-arid climate. The city lies between 22°13'00"N and 22°24'00"N latitude, and 70°44'00" E and 70°56'00"E longitude. The summers here are hot and dry, and run from March to June. The temperatures during summer often cross 42 °C, and might go beyond 45 °C. The city is located on the banks of the Aji River; however, the river remains dry except during the monsoon period (July to September). Winters start late in November and are mostly pleasant. The city is one of the prime industrial centres of Gujarat state, India. Covering an area of nearly 170 sq km, the city houses a population of 1,286,995 inhabitants as per the 2011. According to Ray et al. (2013), the frequency of heat waves in Rajkot has increased substantially during the decade 2001-10 as compared to earlier decades. The decadal frequency of moderate heat waves oscillated from 2 during 1971-80 to 33 during 2001-10. The years after 2010 have been hotter than before. Therefore, the risk associated to human life due to heat stress in the city cannot be underestimated.

2.3. Bhubaneswar:

Bhubaneswar is the capital city of the Indian state of Odisha, situated between 20°12'00"N and 20°21'00"N latitude, and 85°44'00" E and 85°55'00"E longitude. It is located on the Eastern Ghats, about 40 km west of the Bay of Bengal (with an average elevation of 45 meters above mean sea level) in Khordha district. It lies on the west bank of the River Kuakhai, which is a tributary of the River Mahanadi that flows about 30 km southeast of Cuttack. The river Daya branches off at Kathjodi and flows along the southeastern part of the city. The city has a spatial spread of 135 sq. km with 67 Census wards and a population of more than 8 Lakhs (as per the 2011 census). It has a population density of 6,228 persons/ sq km. The city registered a growth rate of 176.67% during 1961-71, which was the highest in India for that period. The decadal growth rate of the city is very high at 30.2%. Bhubaneswar has become one of the hottest Indian cities with scorching summers in recent times. Extremely high increase in average monthly mean maximum temperature, continuous increase in the number of hot days and rising temperature difference between Bhubaneswar and

the nearby cities provide an impression of gradual emergence of the city as an urban heat island. The city in the past has recorded a history of heat waves in 1998, 2002, 2004 and 2008. Though the city also gets impacted by various other disasters (such as cyclones), heat waves have emerged as a recurring threat, which gets exacerbated due to increasing urbanisation.

3. Methodology

Following steps were followed to obtain the hotspot maps:

Step 1: Data Identification:

For the purpose of developing the Heat Stress Action Plans at ward level for Bhubaneswar, Delhi and Rajkot, it was crucial to identify the datasets which can be used for ward level mapping. A comparative assessment of satellite datasets available for the purpose was done (Table 1). After screening, we decided to use Landsat satellite data, in particular Landsat-8 data. Landsat-8 provides a range of open source data at a spatial resolution of 30 m. This satellite has two instruments: OLI (Operational Land Imager) and TIRS (Thermal Infrared Sensor). Landsat 8 provide data in 11 spectral bands, out of which two are thermal bands (What are the band designations for the Landsat satellites?, 2019). Though the data in thermal bands are collected at 100 m resolution, it is resampled to 30 m by the United States Geological Survey (USGS) before distributing to users.

Table 1: *Comparative Assessment of Satellite Data Available for Thermal Mapping*

Satellite/Sensor	Spectral Bands	Special Resolution	Temporal Resolution
Landsat 8 OLI/TIRS	**11 bands**	**30 m**	**16 days, equatorial crossing time around 10 AM**
Kalpana-1	3 bands	8 km (for thermal band), 2 km for rest	23-33 mins
MODIS	36 bands	1 km	1-2 days, equatorial crossing time for Terra 10:30 AM and for Aqua 1:30 PM
ASTER	14 bands	90 m (for thermal band), 15-30 m for rest	16 days, equatorial crossing time around 10:30 AM

AVHRR	6 bands	1-4 km	Twice a day (one in afternoon 1:30-2:30 PM; and other in night 1:30-2:30 AM)

Step 2: Conversion of DNs to Spectral Radiance values:

Satellite imageries with finer spatial resolutions were obtained from LANDSAT 8. The thermal bands, band 10 and band 11, are mostly employed for the purpose of LST retrieval; however, it has been observed that band 11 has more uncertainty than band 10 (Yu et al., 2014). Therefore, band 10 of Landsat 8 data was used for retrieval of LST.

April and May images of Bhubaneswar, Rajkot and Delhi were downloaded from earthexplorer portal of United States Geological Survey (USGS) (USGS, 2019).

The energy recorded by the sensors is converted to Digital Numbers (DN) which is provided to users in the form of satellite data. Therefore, it is important to convert DN to radiance for any further analysis. The value of Top of Atmosphere (TOA) spectral radiance (Lλ) was determined by multiplying multiplicative rescaling factor (0.000342) of TIR (Thermal Infrared) bands with its corresponding TIR band and adding additive rescaling factor (0.1) with it.

$$L\lambda = ML * Qcal + AL \quad \text{(Equation 1)}$$

Where, Lλ - Top of Atmospheric Radiance in watts/ (m^2*srad*μm)

ML - Band specific multiplicative rescaling factor

Qcal - band 10 image

AL - Band specific additive rescaling factor

The spectral radiance thus computed is converted to Brightness Temperature (BT) through following equation (Rajeshwari and Mani, 2014):

$$BT = K2/L\lambda\,[(K1/L\lambda) + 1] \quad \text{(Equation 2)}$$

Where, K1 and K2- thermal conversion constant and

Lλ – Top of Atmospheric spectral radiance.

Step 3: Computation of Land Surface emissivity (LSE) and Land Surface Temperature (LST)

Next step is computation of Land surface emissivity (LSE). The land surface emissivity is indispensable for LST computation from satellite data. The emissivity of land, unlike that of oceans, can differ significantly from unity and vary with vegetation, surface moisture, roughness, and viewing angles. There are several methods to compute LSE. In this case, NDVI (Normalized Difference Vegetation Index) based approach was used to compute LSE because of its simplicity and wider acceptability. The equation to compute LSE is (Rajeshwari and Mani, 2014):

$$LSE\ (\varepsilon)\ = \varepsilon s\ (1 - FVC)\ +\ \varepsilon v\ *\ FVC \qquad \text{(Equation 3)}$$

Where, εs and εv - soil and vegetative emissivity values of the corresponding bands,

FVC – Fractional Vegetation Cover

FVC for an image was calculated by

$$FVC\ =\ NDVI\ -\ NDVIs/\ NDVIv\ -NDVIs \qquad \text{(Equation 4)}$$

Where, NDVIs – NDVI reclassified for soil

NDVIv – NDVI reclassified for vegetation

NDVI is computed from red and near-infrared bands of Landsat 8 OLI data as follows:

$$NDVI\ =\ (NIR\ -\ Red)/\ (NIR\ +\ Red) \qquad \text{(Equation 5)}$$

The LST is now retrieved using the equation (Yu et al., 2014):

LST = γ [ε -1 (Ψ1 BT + Ψ2)+Ψ3] + δ (Equation 6)

The symbols γ, Ψ and δ are coefficients and the equations used to compute these coefficients can be found in Yu et al., 2014.

This entire process has been automatized in Thermal Remote Sensing Tool Box, developed by Walawender et al. (2012). This tool box is compatible with ArcGIS. The tool box was provided by Dr Jakub P Walawender of Institute of Meteorology and Water Management – National Research Institute (IMGW-PIB), Poland.

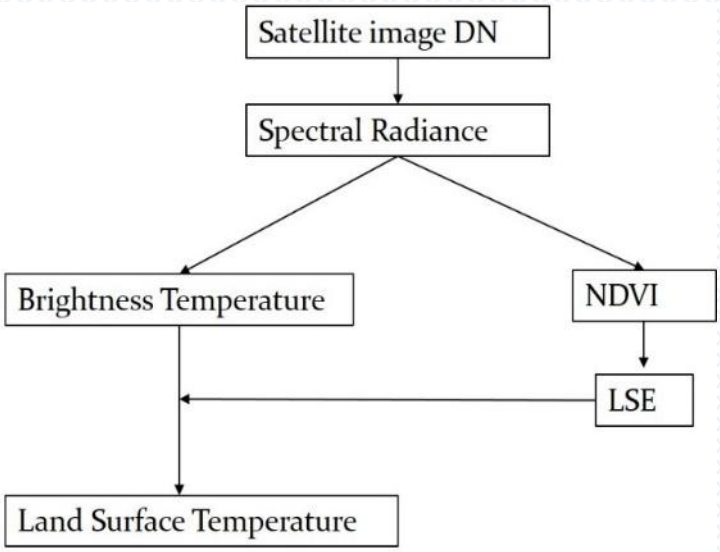

Figure 3: *Flowchart depicting calculation of LST from satellite image*

4. Results and Discussions

4.1. Delhi:

Land Surface Temperature (LST) map was prepared for 30 May 2019 (the day when Delhi recorded a maximum air temperature of 48 degree C), and spatial variability of LST in different municipal zones of Delhi was analysed. The zones Narela and Najafgarh recorded maximum LST of 60.48 degree C and 59.06 degree C (see the LST map shown in Figure 4). The analysis reveals that on 30 May 2019, approximately 1450.05 sq km of land area of Delhi experienced a surface temperature exceeding 40 °C.

The spatial variation of ambient air temperature was also analysed by the maximum air temperature (Tmax) recorded by DPCC (Delhi Pollution Control Committee) monitors (Figure 5) spread across various areas of NCT of Delhi. Here also Narela and Najafgarh recorded high values of Tmax as 47.6 °C and 47.8 °C respectively. 21, out of 24, stations registered Tmax in the range of 45-48 °C. Minimum Tmax was recorded at Panjabi Bagh: 44.5°C whereas Maximum Tmax was recorded at Indira Gandhi International (IGI) Airport: 48 °C. The difference between minimum and maximum Tmax was 3.5 °C.

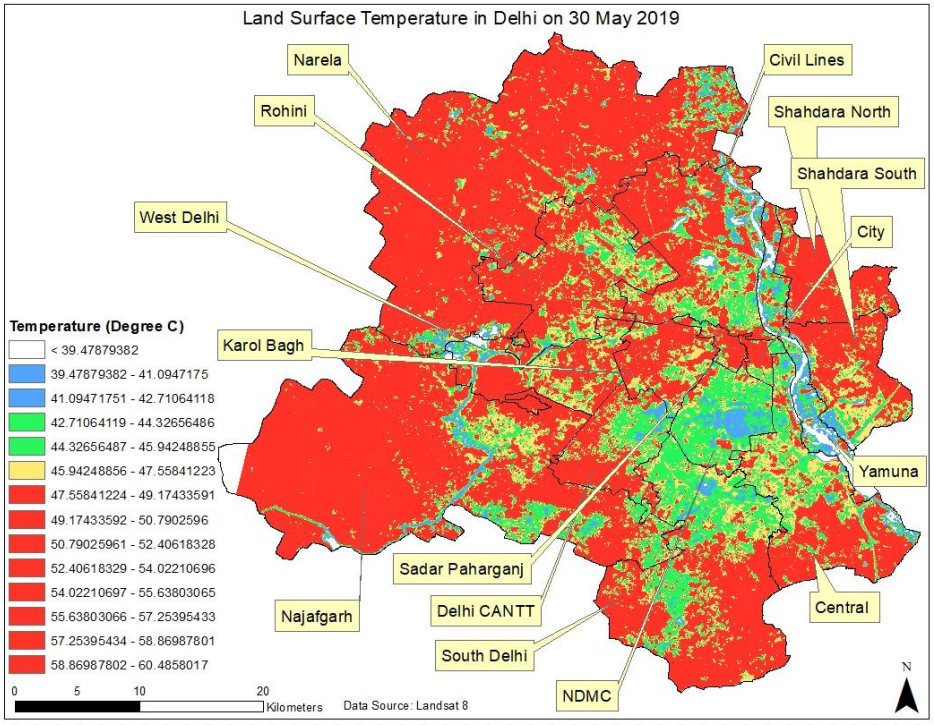

Figure 4: *LST map of Delhi for 30 May 2019*

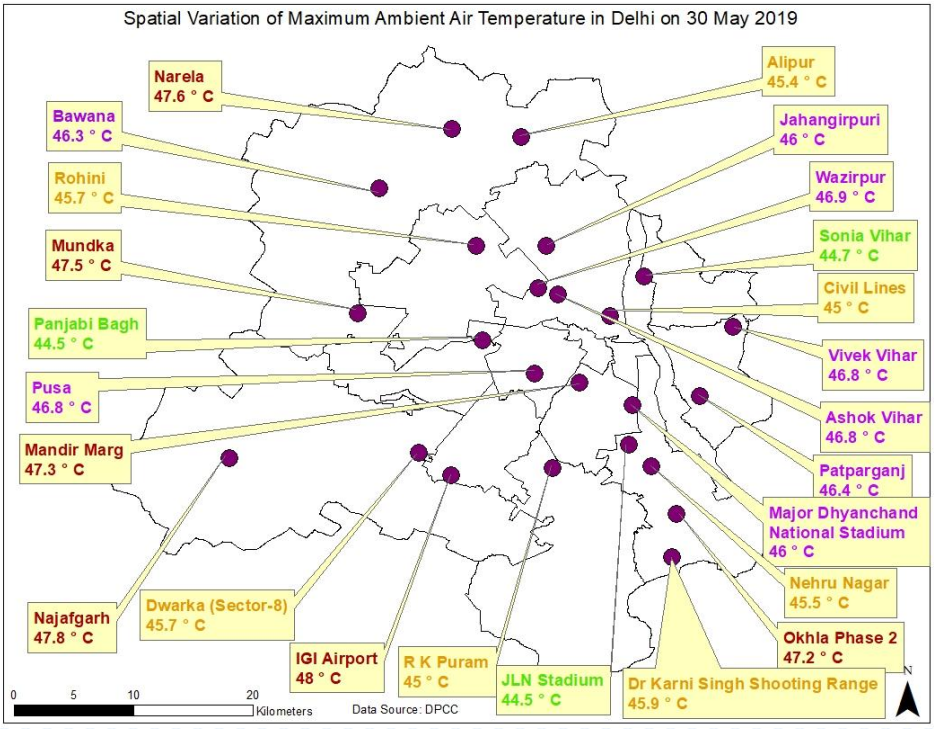

Figure 5*: Spatial variation of maximum ambient air temperature on 30 May 2019 as per the data recorded by DPCC monitors*

In addition, LST maps were prepared using satellite data of 06 April 2017, 27 May 2018 and 12 June 2018 (Figure 6). Using all these maps, thermal hotspots were identified as the areas having LST more than 40 °C. One such map for 06 April 2017 is shown in Figure 7. 10 such hotspots were selected based on their proximity to slums and surveyed on ground (Table 2) for assessing the socio-economic impacts of heat stress on vulnerable population living in these areas. Slums were considered as the agglomeration of vulnerable population in the city for assessing the impacts of heat stress.

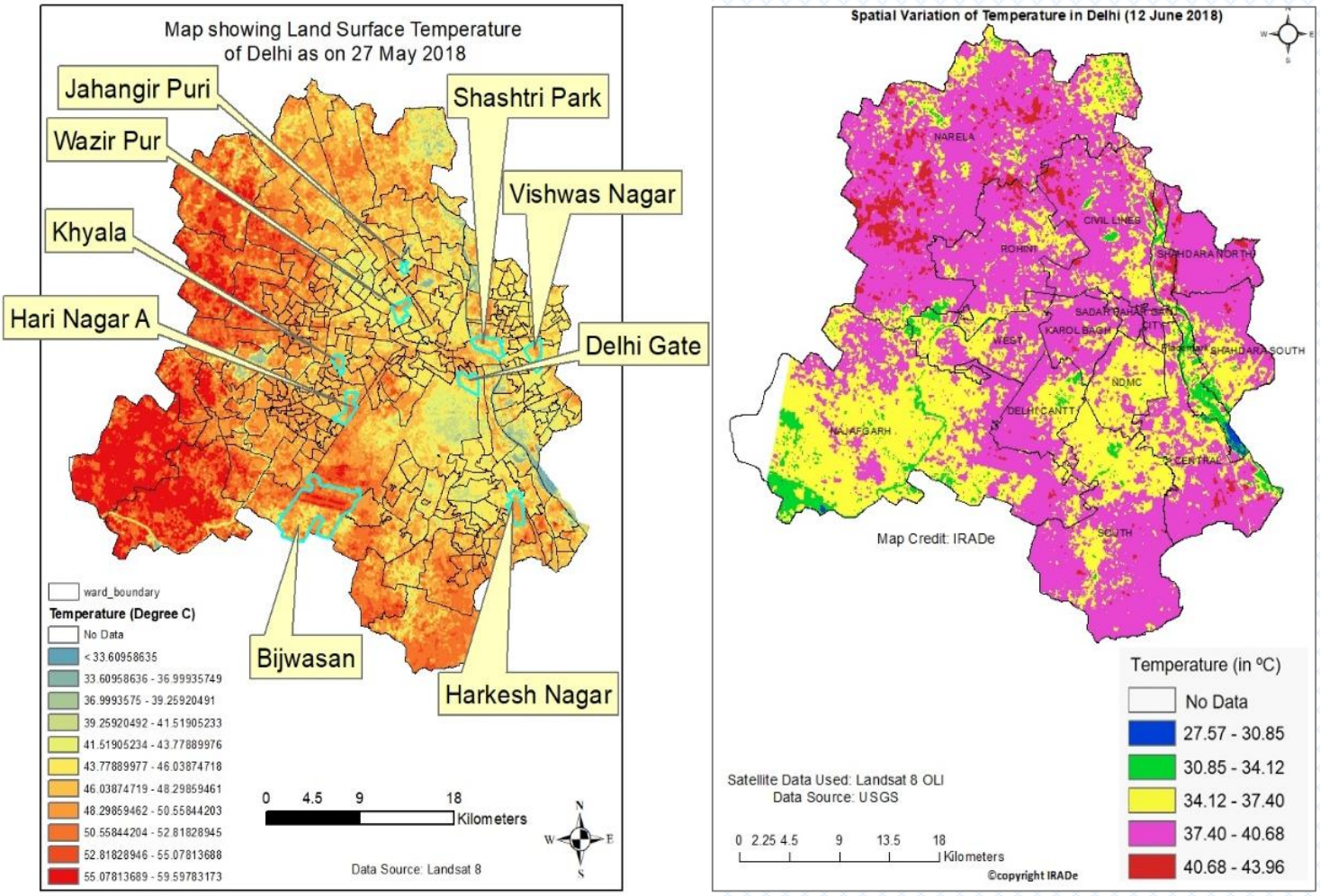

Figure 6: *LST maps of Delhi for 27 May 2018 and 12 June 2018*

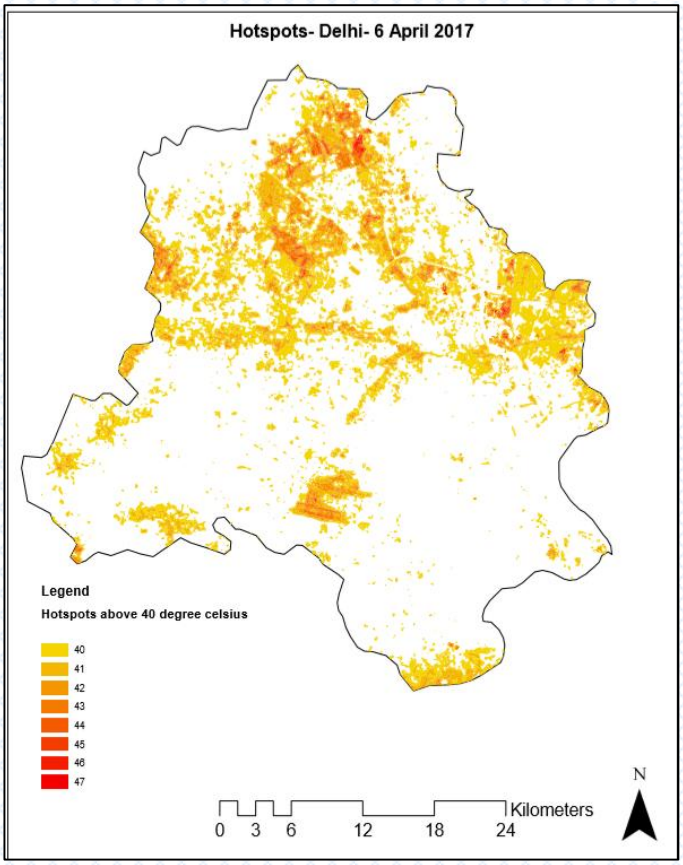

Figure 7: *Map showing hotspots above 40° C in Delhi on 6 April 2017*

Table 2: *Thermal hot-spots surveyed in Delhi based on LST maps*

S .NO.	Surveyed Hotspots	New Ward Name/ No.
1	Indira kalyan Vihar	HARKESH NAGAR 092S
2	Sanjay colony Okhla phase 2	HARKESH NAGAR 092S
3	Slum in Khayala	KHYALA 008S
4	Prem bari Bridge	WAZIR PUR 072N
5	Slum near Samalkha	BIJWASAN 048S
6	New Sanjay Amar colony, Vishwas nagar	VISHWAS NAGAR 017E
7	Mayapuri slum along Rewari railway line	HARINAGAR A 010S
8	Jahangirpuri	JAHANGIR PURI 021N
9	Shakoor ki Dandi	DELHI GATE 088N
10	Buland masjid slums	SHASTRI PARK 025E

4.2. Rajkot:

For Rajkot, Landsat 8 data of May and June months of 2017 and 2018 were employed to map LST. For 2017, data of 04 May and 14 June were used, whereas, for 2018, data of 07 May and 08 June were used (Figure 8 and 9).

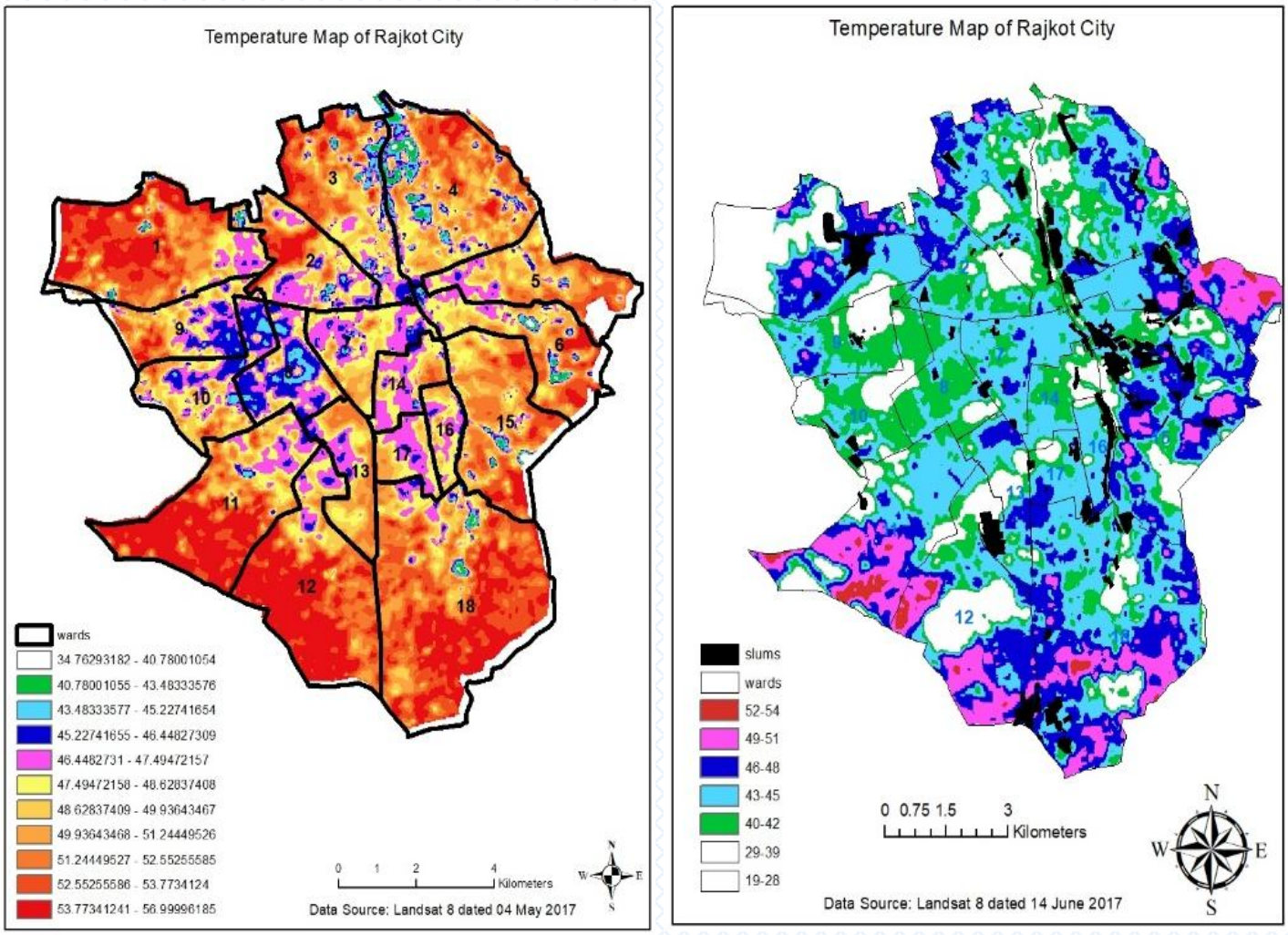

Figure 8: *LST distribution in Rajkot on, 04 May and 14 June,2017*

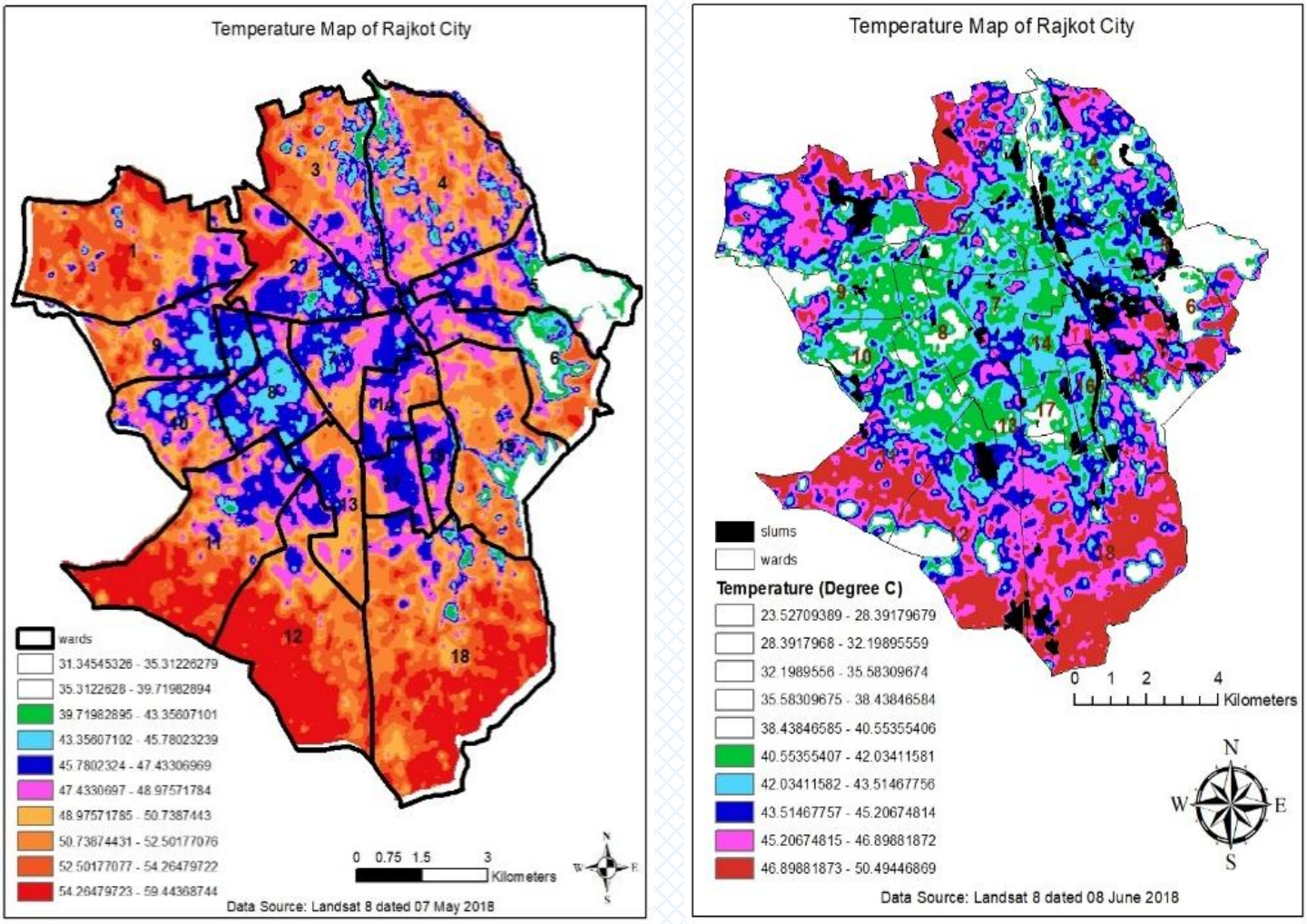

Figure 9: *LST distribution in Rajkot on, 07 May and 08 June, 2018*

Slum distribution in Rajkot was also mapped, and slum distribution map was overlaid on LST maps to identify vulnerable thermal hotspots. The locations of AWS installed by RMC was also mapped and together a map showing slums and AWS locations were developed (Figure 10). All these layers were collectively used to identify areas for ground visits in Rajkot (Figure 11 and 12). As the temperatures during peak summers often cross 42 °C, we considered areas with LST 42 °C or more as the hotspots.

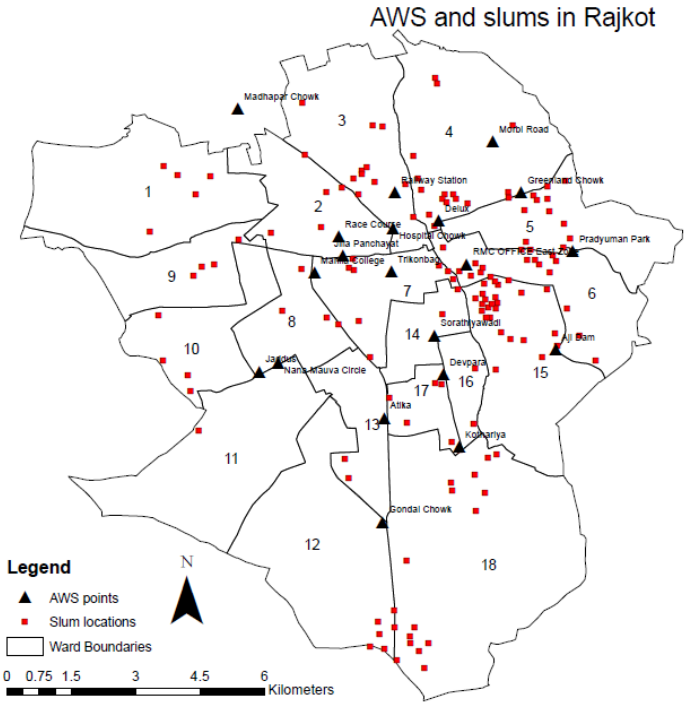

Ward Number	Number of slums
1	5
2	4
3	12
4	16
5	13
6	18
7	8
8	4
9	4
10	4
11	1
12	6
13	2
14	2
15	23
16	2
17	5
18	16

AWS NAME	Ward No.
Jilla Panchayat	7
Greenland Chowk	5
Madhapar Chowk	_
Railway Station	3
Nana Mauva Circle	11
Mahila College	8
Delux	6
Jaddus	11
RMC OFFICE East Zone	6
Race Course	2
Atika	13
Aji Dam	15
Sorathiyawadi	14
Kothariya	18
Gondal Chowk	12
Morbi Road	4
Hospital Chowk	2
Devpara	17
PradyumanPark	6
Trikonbag	7

Figure 10: *Map showing AWS and slum locations in Rajkot*

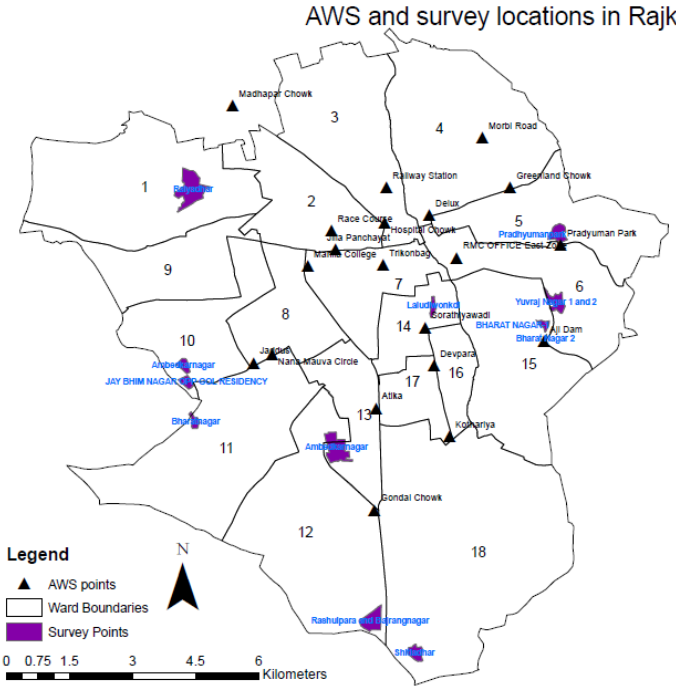

Survey Locations	Ward No.
Ambedkar Nagar	13
Rashulpura and Bajrangnagar	12
Rajyadhar	1
Shitaldhar	18
Jay Bhim Nagar	10
BhimRav nagar	5
Bharat Nagar 1	15
Bharat Nagar	11
Pradyuman park	5
Laludiwonkdi	14

AWS NAME	Ward No.
Jilla Panchayat	7
Greenland Chowk	5
Madhapar Chowk	_
Railway Station	3
Nana Mauva Circle	11
Mahila College	8
Delux	6
Jaddus	11
RMC OFFICE East Zone	6
Race Course	2
Atika	13
Aji Dam	15
Sorathiyawadi	14
Kothariya	18
Gondal Chowk	12
Morbi Road	4
Hospital Chowk	2
Devpara	17
PradyumanPark	6
Trikonbag	7

Figure 11: *Survey locations in Rajkot*

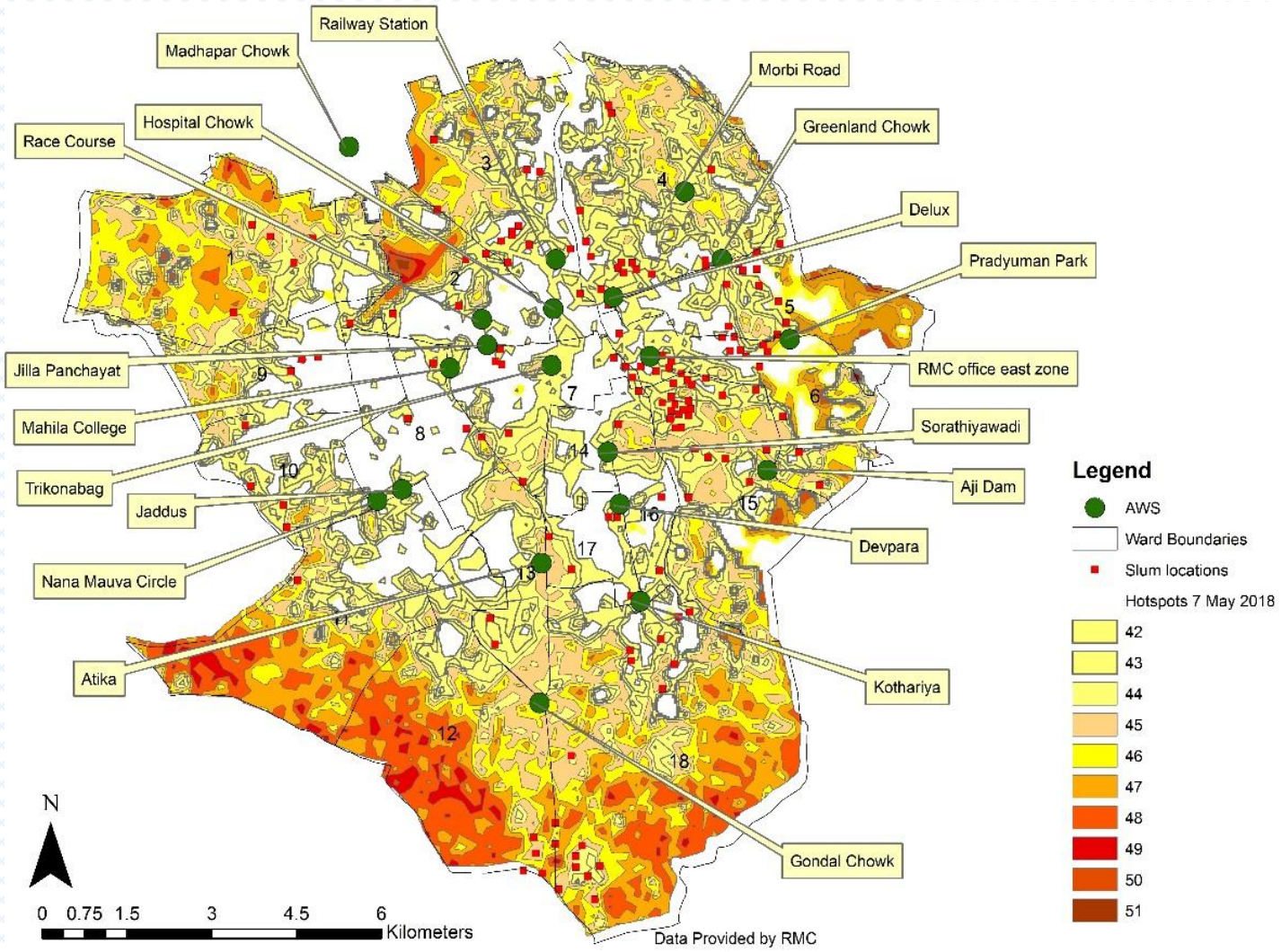

***Figure 12**: Thermal hotspots in Rajkot with LST =/> 42 °C*

4.3. Bhubaneswar:

LST maps for Bhubaneswar were prepared using satellite data of 12 April 2017 and 14 May 2017 (Figure 13) and thermal hotspots in Bhubaneswar were identified as the areas having LST 40 °C or more.

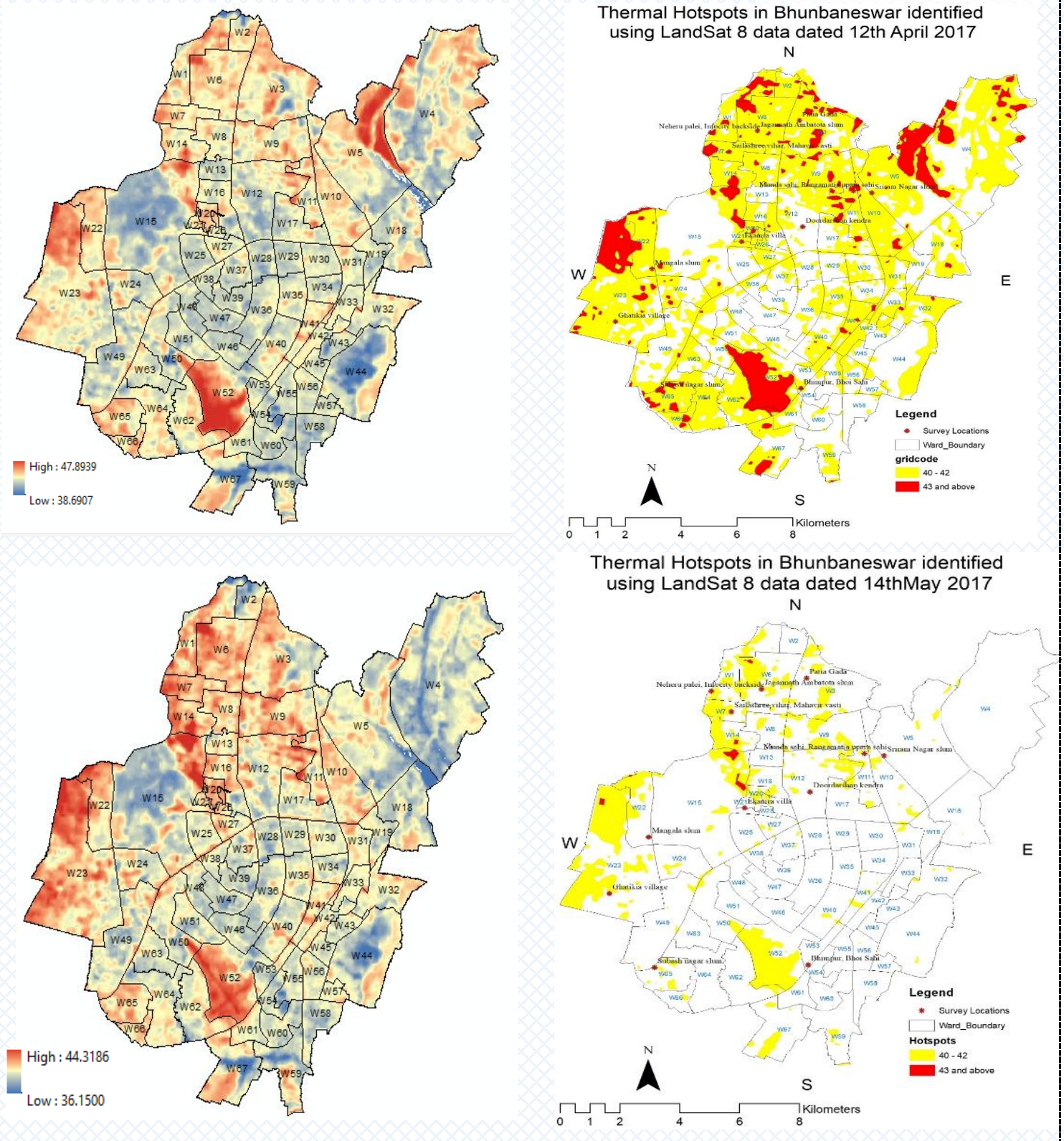

Figure 13: *LST and hotspot maps for Bhubaneswar for 12 April 2017 (above) and 14 May 2017 (below)*

The hotspots identified were ward numbers: 1,3, 5, 6, 7, 9, 12, 15, 20, 23, 52 and 65. In each of these wards, locations with vulnerable populations were identified and surveyed (Table 3).

Table 3: *Thermal hotspots surveyed in Bhubaneswar*

Surveyed Hotspots	Ward Number
Neheru palei, Infocity backside	1
Patia Gada	3
Sriram Nagar slum	5
Jagannath Ambatota slum	6
Sailashree vihar, Mahavir vasti	7
Munda sahi, Rangamatia upara sahi	9
Doordarshan kendra	12
Ekamra villa	15
Bhimpur, Bhoi Sahi	52
Ghatikia village	23
Mangala slum	20
Subash nagar slum	65

As there was just one IMD station in Bhubaneswar, ambient air temperature was recorded on ground in all the above locations using hand-held Psychrometers. The maps prepared for dry-bulb and wet-bulb temperature and RH in Bhubaneswar for 09 May 2018 is shown in Figure 14.

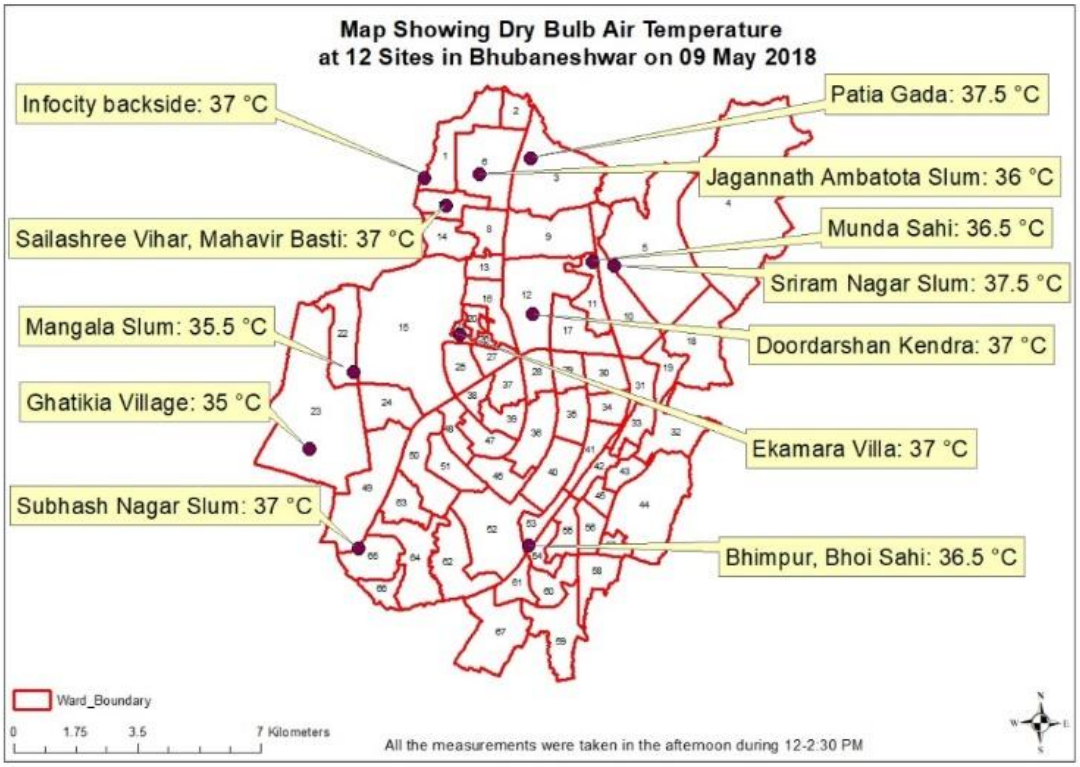
Map Showing Dry Bulb Air Temperature
at 12 Sites in Bhubaneshwar on 09 May 2018
Infocity backside: 37 °C
Patia Gada: 37.5 °C
Jagannath Ambatota Slum: 36 °C
Sailashree Vihar, Mahavir Basti: 37 °C
Munda Sahi: 36.5 °C
Sriram Nagar Slum: 37.5 °C
Mangala Slum: 35.5 °C
Doordarshan Kendra: 37 °C
Ghatikia Village: 35 °C
Ekamara Villa: 37 °C
Subhash Nagar Slum: 37 °C
Bhimpur, Bhoi Sahi: 36.5 °C
Ward_Boundary
0 1.75 3.5 7 Kilometers
All the measurements were taken in the afternoon during 12-2:30 PM

(a)

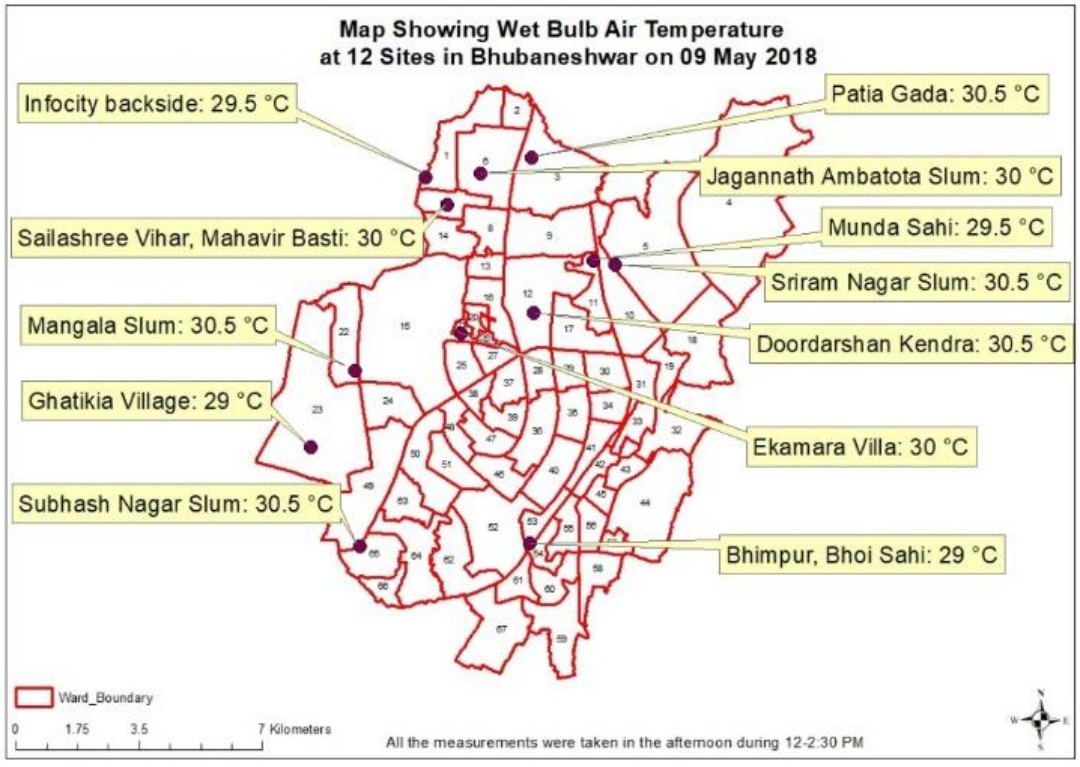
Map Showing Wet Bulb Air Temperature
at 12 Sites in Bhubaneshwar on 09 May 2018
Infocity backside: 29.5 °C
Patia Gada: 30.5 °C
Jagannath Ambatota Slum: 30 °C
Sailashree Vihar, Mahavir Basti: 30 °C
Munda Sahi: 29.5 °C
Sriram Nagar Slum: 30.5 °C
Mangala Slum: 30.5 °C
Doordarshan Kendra: 30.5 °C
Ghatikia Village: 29 °C
Ekamara Villa: 30 °C
Subhash Nagar Slum: 30.5 °C
Bhimpur, Bhoi Sahi: 29 °C
Ward_Boundary
0 1.75 3.5 7 Kilometers
All the measurements were taken in the afternoon during 12-2:30 PM

(b)

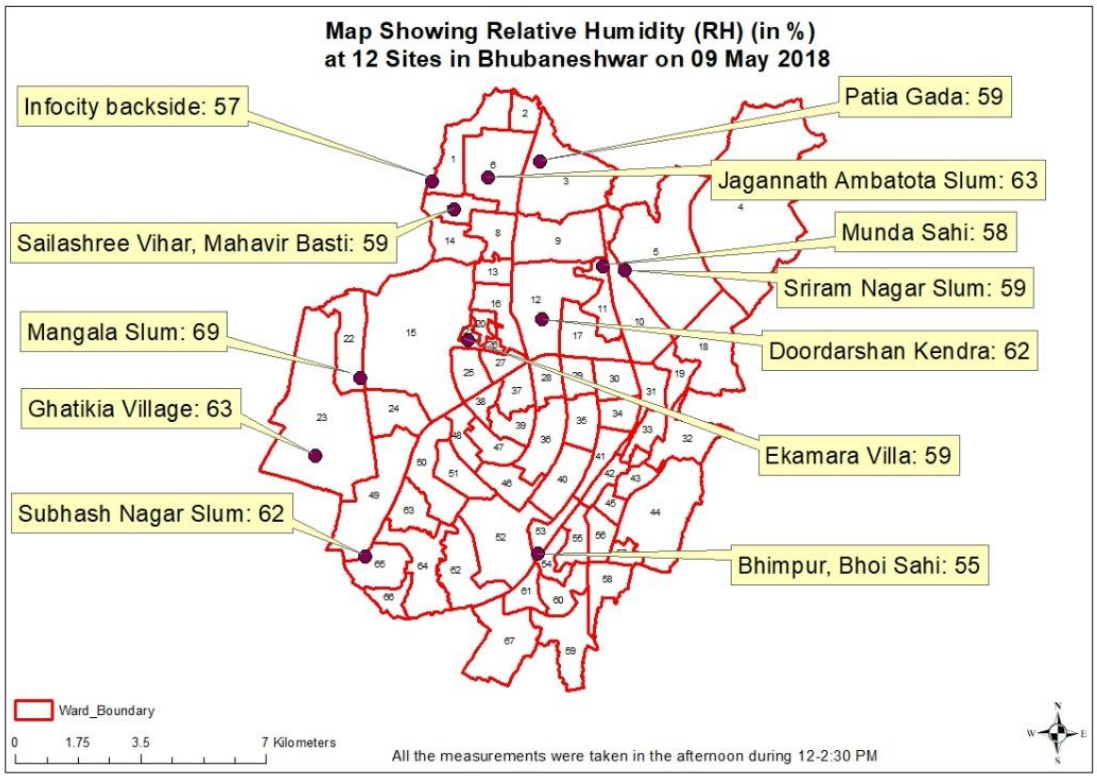

(c)

Figure 14: *Maps showing dry-bulb air temperature (a), wet-bulb temperature (b) and RH (c) measured in Bhubaneswar on 09 May 2018*

Some of these sites were again surveyed in 2019 (10 March and 26 March) for recording air temperature (both dry-bulb and wet-bulb) and relative humidity (RH) at 10:30 AM and 2:30 PM (Figure 15, 16, 17, 18, 19, 20). These dates were selected as these dates coincide with satellite overpass dates over the city. For both these dates, LST maps were also prepared using satellite data (Figure 21, 22).

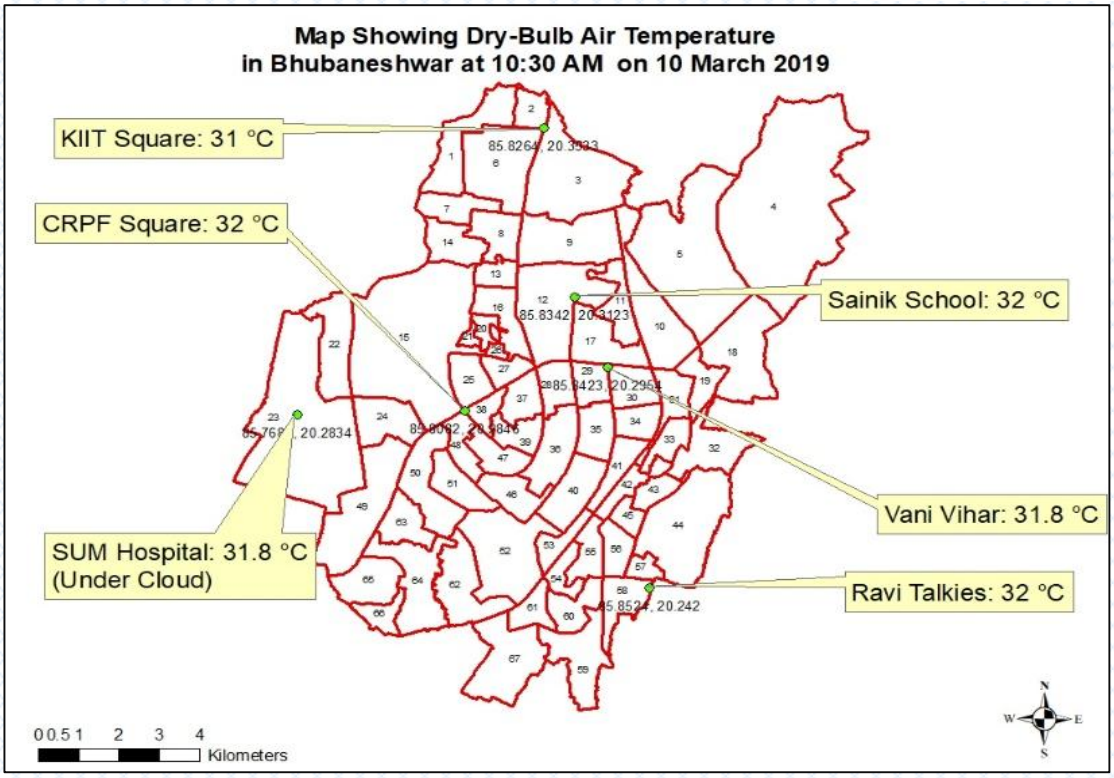

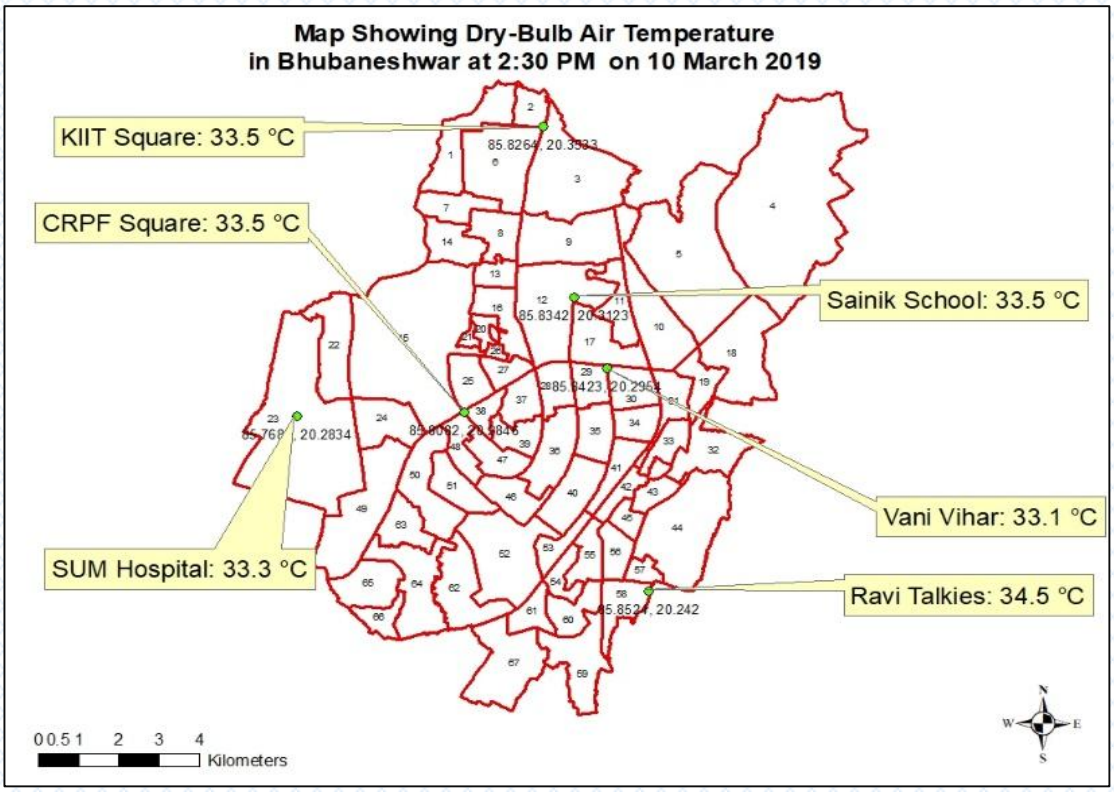

Figure 15: *Dry bulb air temperature recorded in Bhubaneswar at 10:30 AM and 2:30 PM on 10 March 2019*

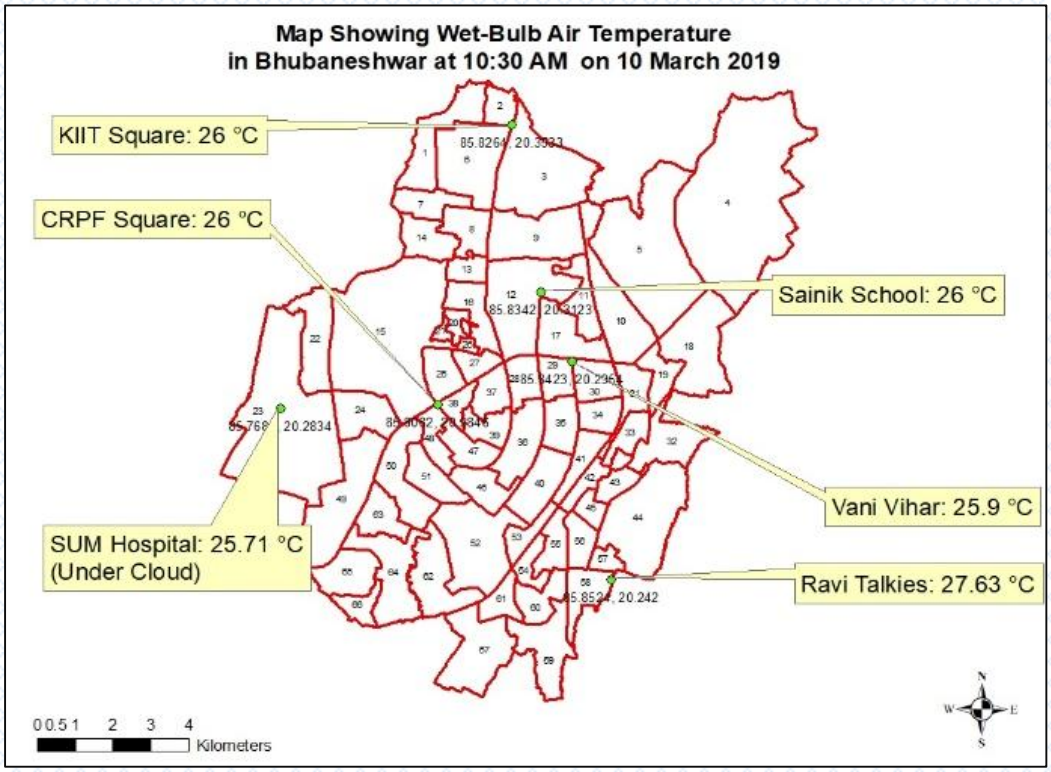

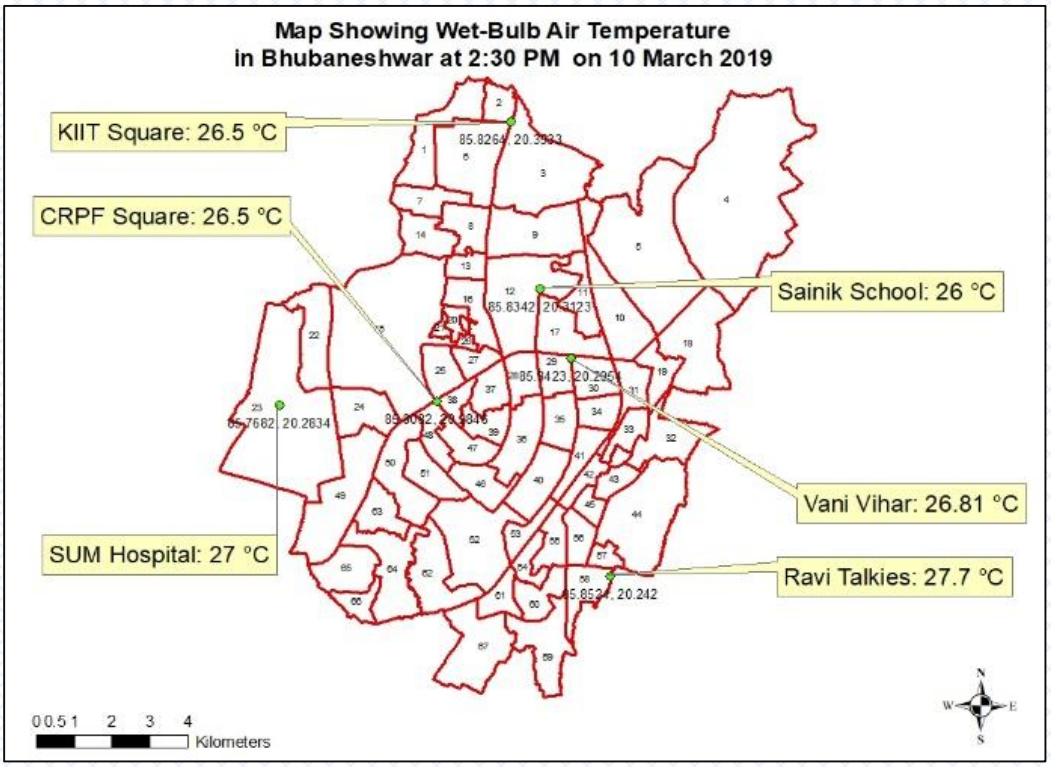

Figure 16: *Map showing wet-bulb air temperature measured at several locations in Bhubaneswar on 10 March 2019 at 10:30 AM and 2:30 PM*

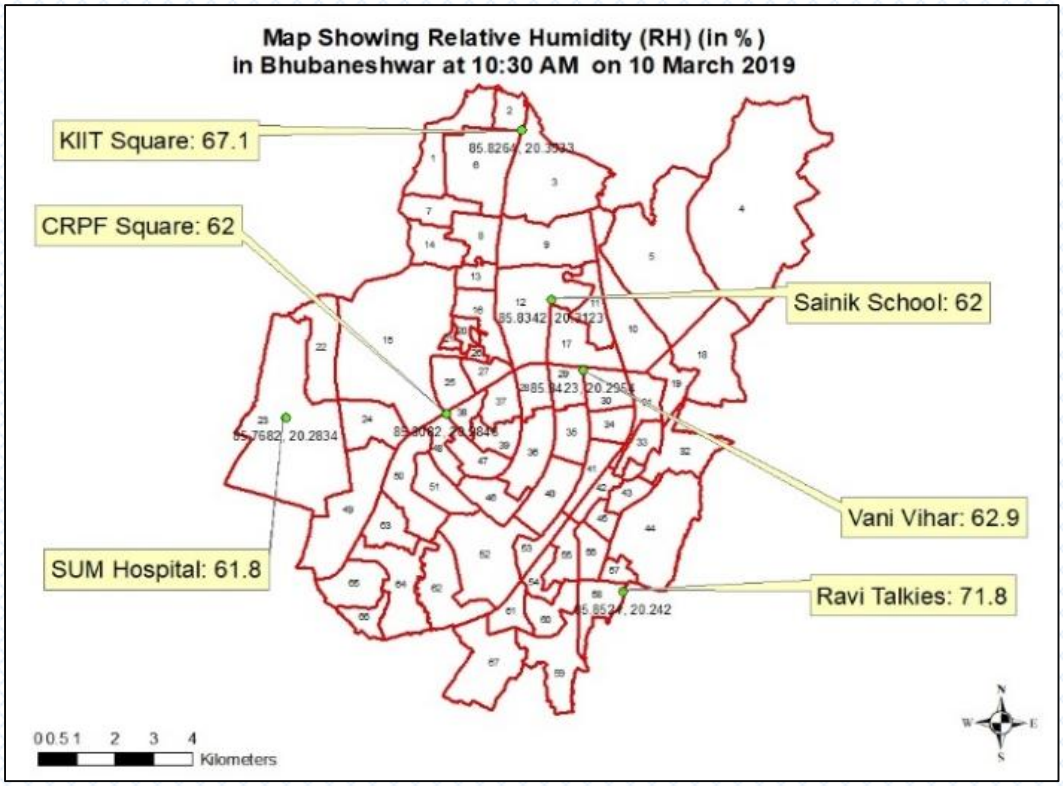

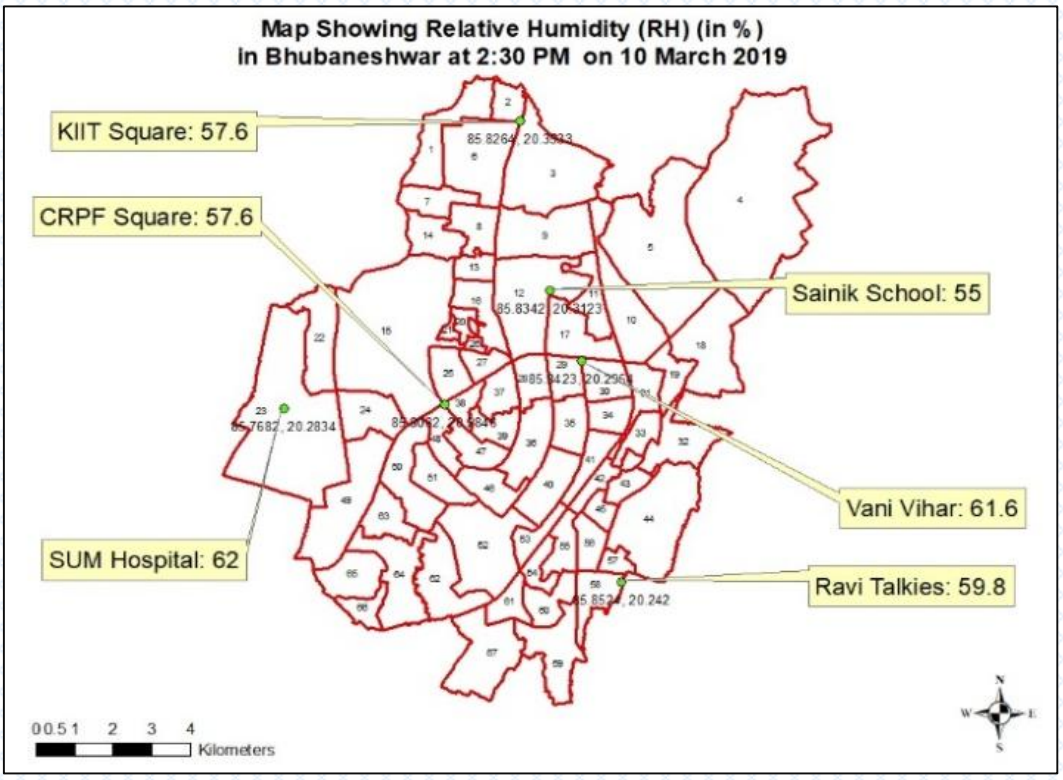

Figure 17: *Maps showing RH at surveyed locations in Bhubaneswar as on 10 March 2019 at 10:30 AM and 2:30 PM*

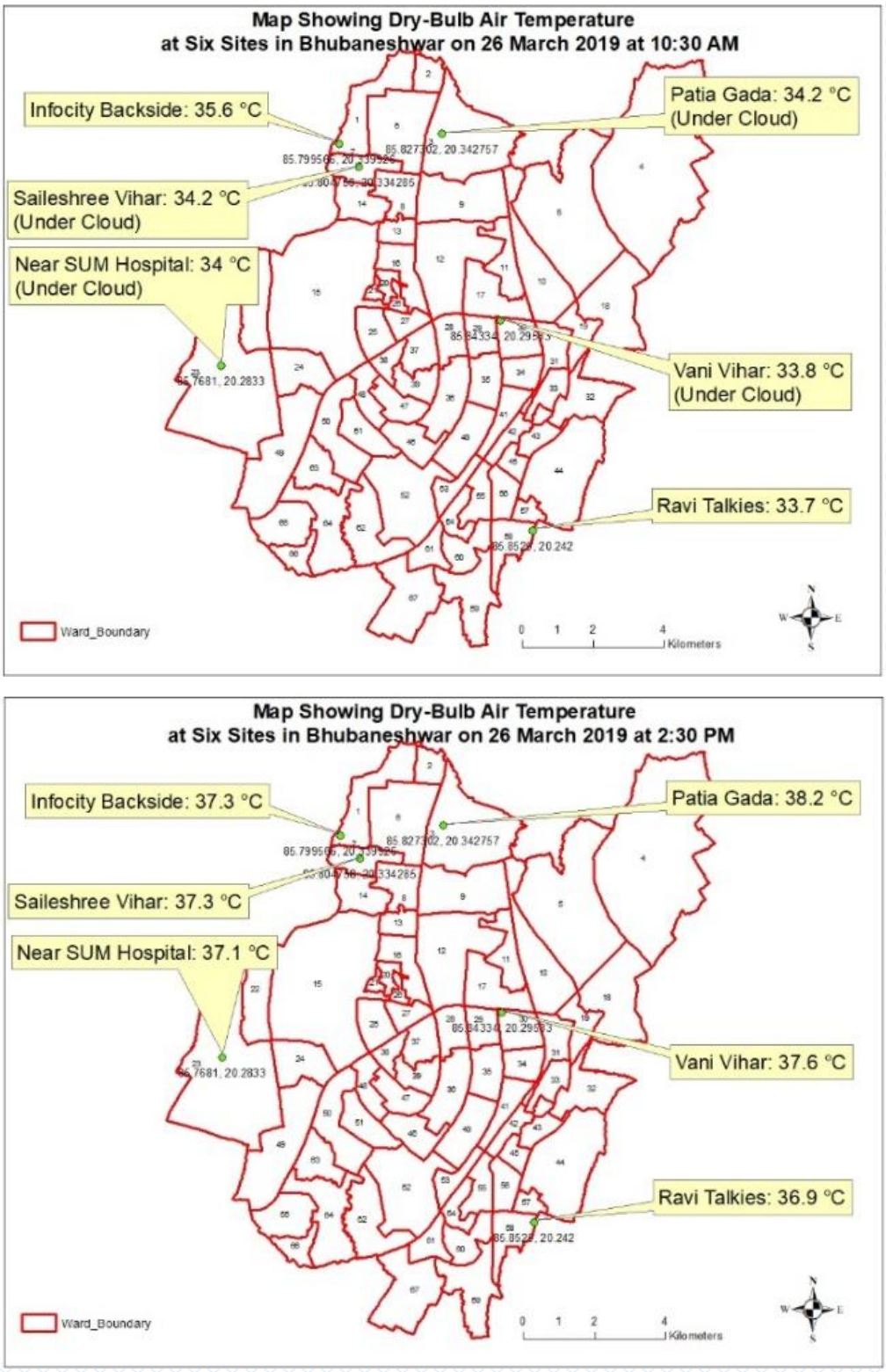

Figure 18: *Dry bulb air temperature recorded in Bhubaneswar at 10:30 AM and 2:30 PM on 26 March 2019*

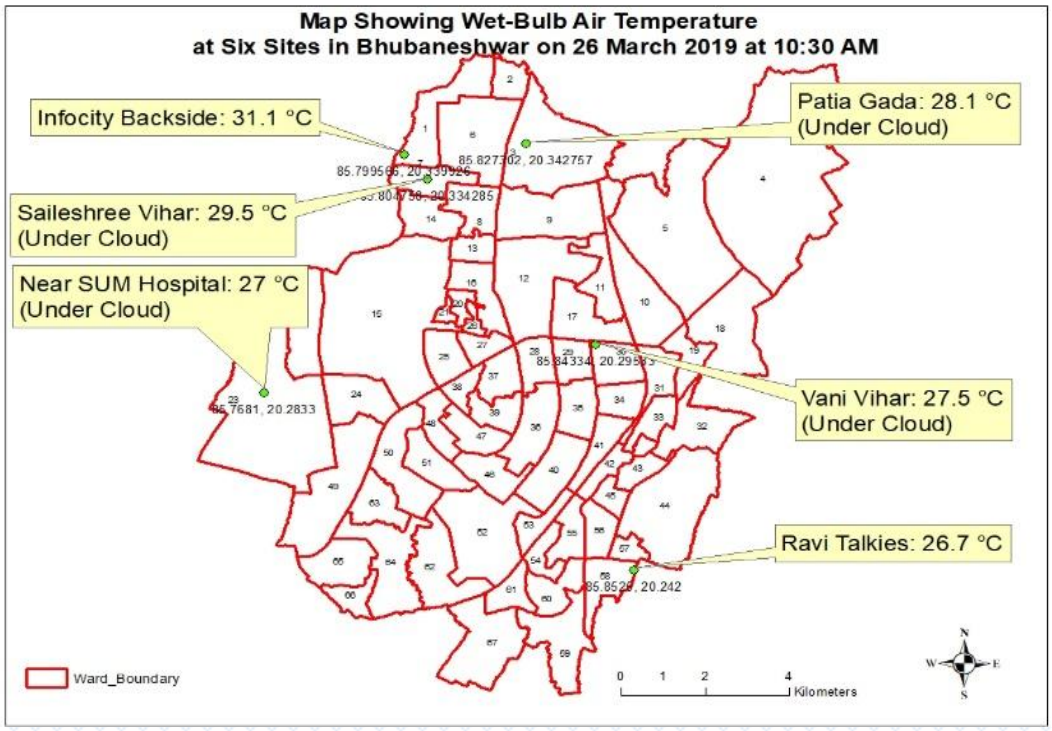

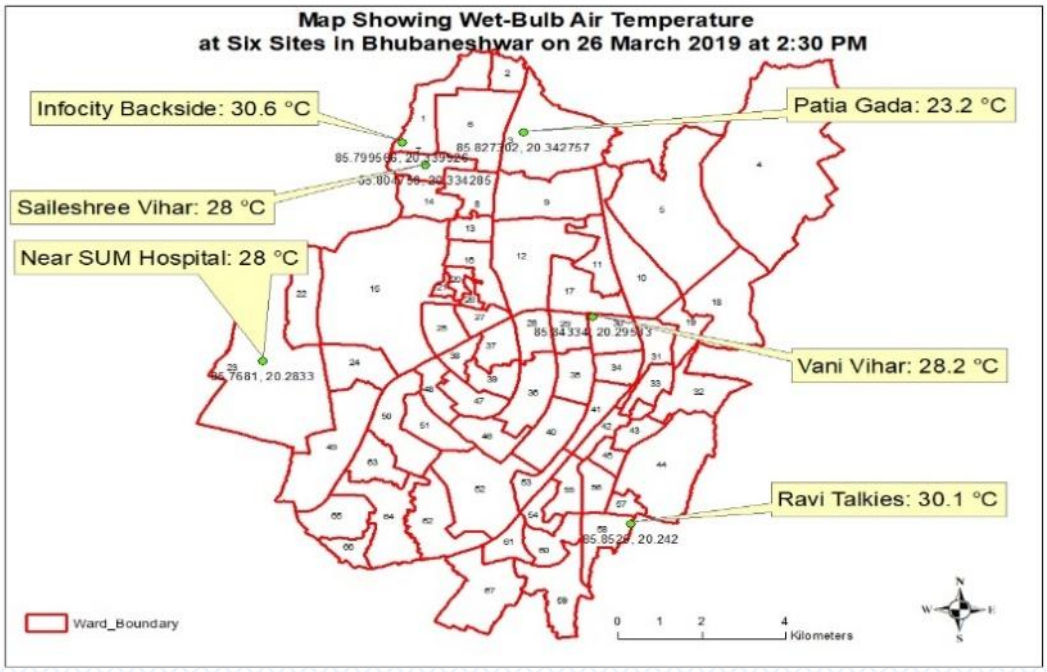

Figure 19: *Map showing wet-bulb air temperature measured at surveyed locations in Bhubaneswar on 26 March 2019 at 10:30 AM and 2:30 PM*

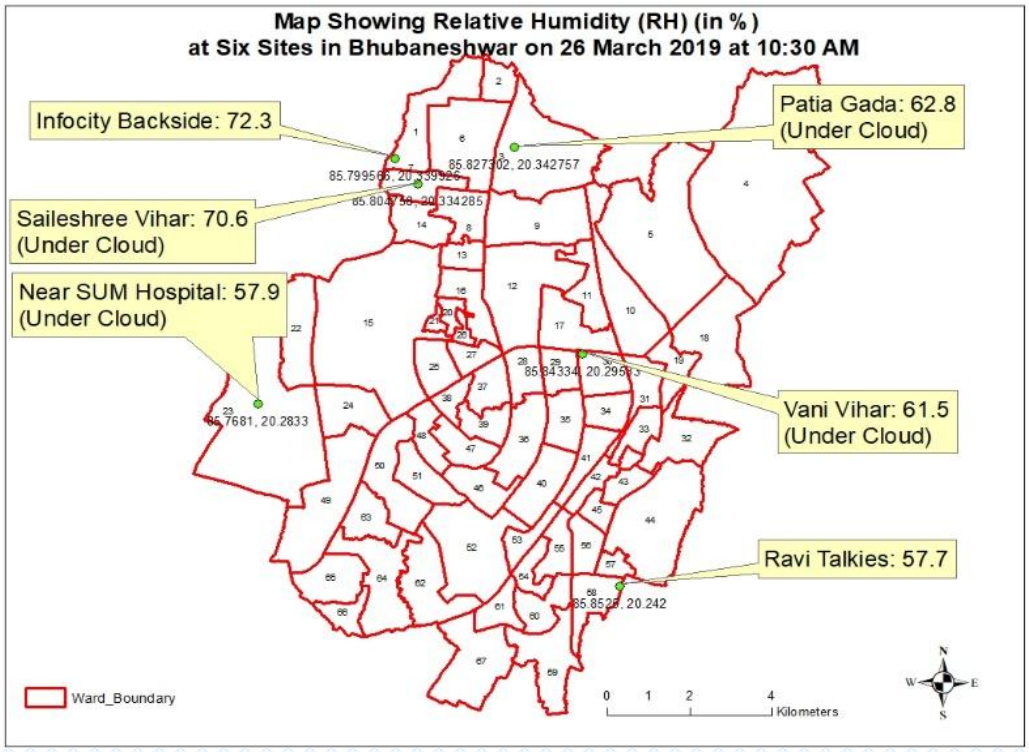

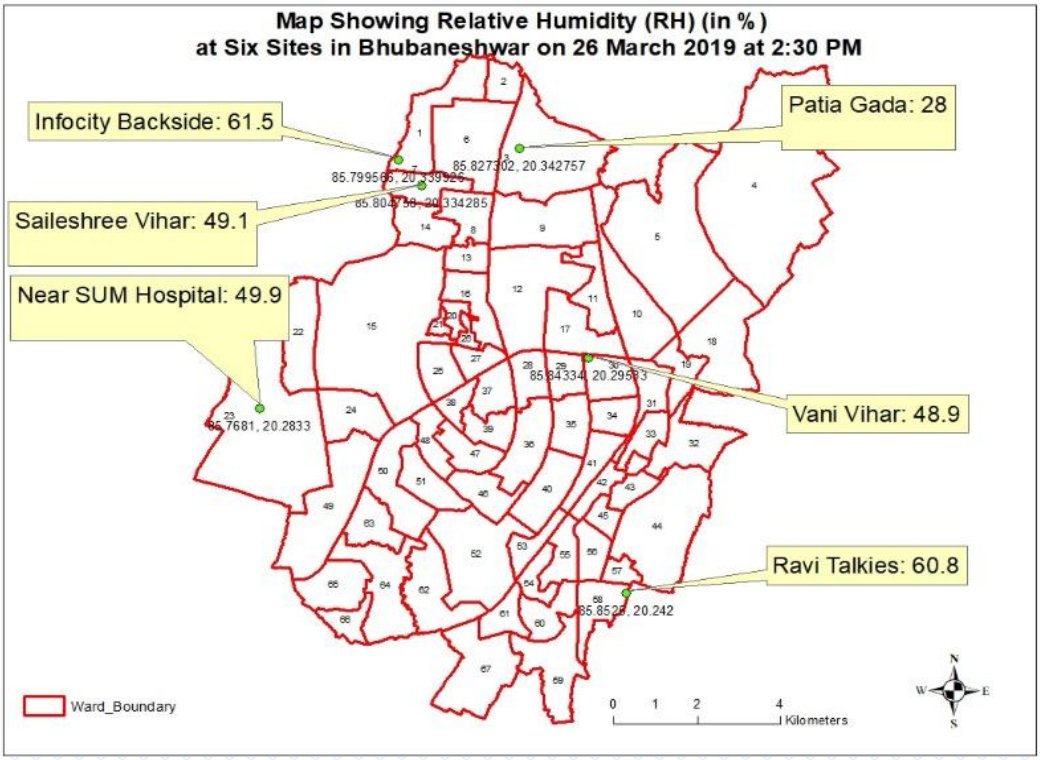

Figure 20: *Maps showing RH at surveyed locations in Bhubaneswar as on 26 March 2019 at 10:30 AM and 2:30 PM*

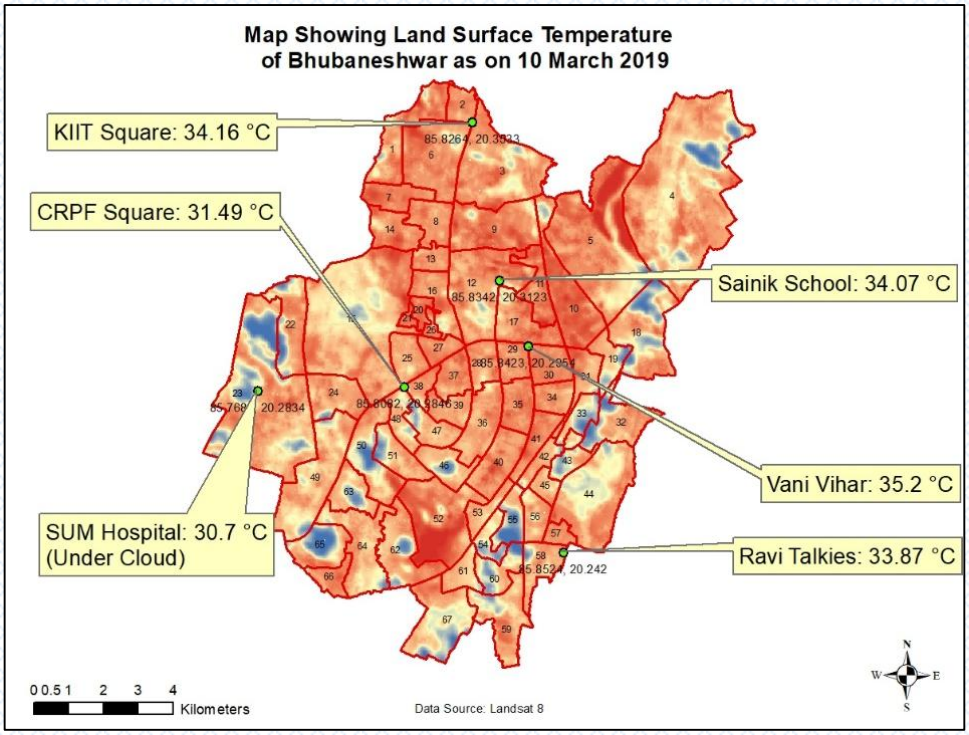

Figure 21: *Map showing LST of Bhubaneswar as on 10 March 2019. The LST of surveyed locations has been highlighted separately.*

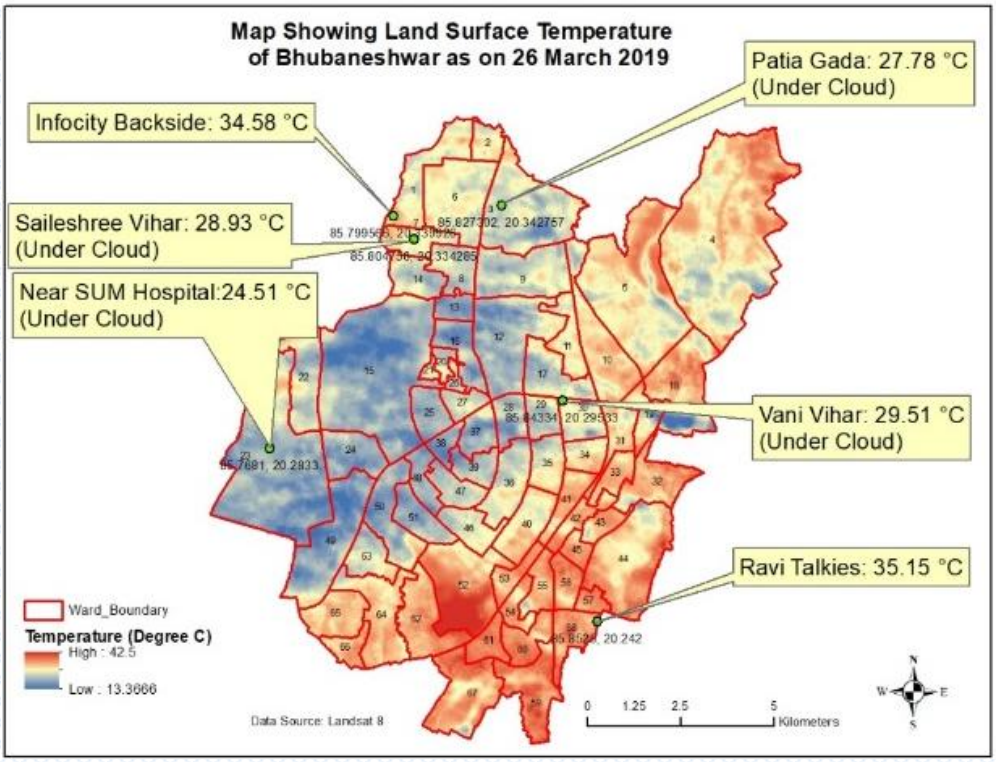

Figure 22*: Map showing LST of Bhubaneswar as on 26 March 2019. The LST of surveyed locations has been highlighted separately.*

5. Conclusion

In this report, we have documented the analysis carried out for identifying the thermal hotspots in three Indian cities, *viz.*, Delhi, Rajkot and Bhubaneswar, using Landsat-8 satellite data. The thermal hotspots were identified at ward-level. Selection of appropriate satellite data for the purpose was an important pre-requisite for this exercise. Landsat-8 provides a record of thermal images since 2013 which are provided at a spatial resolution sufficient enough for ward-level mapping. In addition, this satellite acquires 550 scenes per day, which increases the possibility of getting a cloud-free scene (NASA, 2019). Obtaining a cloud-free scene was also very important for our purpose, and the satellites with fewer scene acquisitions pose more challenges. Even with Landsat-8, we encountered challenges in obtaining a scene for our study area that is completely cloud-free. However, we feel, Landsat-8 so far is better option than any other openly available satellite data in terms of its resolution and availability of images from yesteryears. The hot-spot maps of the three cities will be very useful for policy-makers and city administrators in analysing the local factors contributing to heat-stress in different wards and devising mitigation options to reduce heat stress in these areas within the cities.

6. References:

1. United Nations, (2018). World Urbanization Prospects: 2018 revision. https://www.un.org/development/desa/publications/2018-revision-of-world-urbanization-prospects.html. Accessed on 23 October 2019.
2. dos Santos, A. R.; de Oliveira, F. S.; da Silva, A. G.; Gleriani, J. M.; Gonçalves, W., Moreira, G. L.; Felipe Gimenes Silva et. al (2017). Spatial and Temporal Distribution of Urban heat Islands. *Science of the Total Environment*, 605-606, pp 946-956.
3. Simwanda, M.; Ranagalage, M.; Estoque, R. C.; and Murayama, Y. (2019). Spatial Analysis of Surface Urban Heat Islands in Four Rapidly Growing African Cities. *Remote Sensing*, 11, 1645, pp 1-20.
4. Buyantuyev, A. and Wu, J. (2010). Urban Heat Islands and Landscape Heterogeneity: Linking Spatiotemporal Variations in Surface Temperatures to Land-cover and Socioeconomic Patterns. *Landscape Ecology*, 25, pp 17–33.
5. Sharma, R.; Hooyberghs, H.; Lauwaet, D. and De Ridder, K. (2019). Urban Heat Islands and Future Climate Change – Implications for Delhi's Heat. *Journal of Urban Health*, 96 (2), pp 235-251.

6. IPCC (2013). Climate Change 2013: the physical science basis. Contribution of working group I to the fifth assessment report of the intergovernmental panel on climate change. Cambridge, United Kingdom and New York, NY, USA: Cambridge University Press; 2013.
7. Attri, S. and Tyagi, A. (2010). Climate profile of India. Contribution to the Indian network of climate change assessment (NATIONAL COMMUNICATION-II). Ministry of Environment and Forests, Government of India, 1501, pp 1–129.
8. Mishra, V.; Mukherjee, S.; Kumar, R. and Stone, D. A. (2017). Heat wave exposure in India in current, 1.5 ◦C, and 2.0 ◦C worlds. *Environmental Research Letters*. 12, pp 1-9.
9. Rohini, P.; Rajeevan, M. & Srivastava, A. K. (2016). On the Variability and Increasing Trends of Heat Waves over India. Scientific Reports. 6:26153, pp 1-9.
10. Pai, D. S., Nair, S. A and Ramanathan, A. N. (2013). Long term climatology and trends of heat waves over India during the recent 50 years 1961−2010. *Mausam*. 64, pp 585–604.
11. NASA Earth Observatory, 2019, https://earthobservatory.nasa.gov/images/145167/heatwave-in-india, page accessed on 24 October 2019.
12. Emergency Events Database (EM-DAT). UCLouvain/CRED, Brussels, Belgium. Available at: https://www.emdat.be/ (accessed in 2019).
13. Zhang, Y. and Cheng, J. (2019). Spatio-Temporal Analysis of Urban Heat Island using Multisource Remote Sensing Data: A Case Study in Hangzhou, China. *IEEE Journal of Selected Topics in Applied Earth Observations and Remote Sensing*. DOI: 10.1109/JSTARS.2019.2926417.
14. Wang, Y.; Zhan, Q. and Ouyang, W. (2017). Impact of Urban Climate Landscape Patterns on Land Surface Temperature in Wuhan, China. *Sustainability*. 9, 1700, pp 1-16.
15. Jin, M. S. (2012). Developing an index to measure Urban heat island effect using satellite land skin temperature and land cover observations. *Journal of Climate*. 25 (18), pp. 6193–6201.
16. Li, Y.; Zhang, H. and Kainz, W. (2012). Monitoring Patterns of Urban Heat Islands of the Fast-growing Shanghai Metropolis, China: Using time-series of Landsat TM/ETM+ data," International Journal of Applied Earth Observation and Geoinformation. 19 (10), pp. 127–138.
17. Yuan, F. and Bauer, M. E. (2007). Comparison of Impervious Surface Area and Normalized Difference Vegetation Index as Indicators of Surface Urban Heat Island Effects in Landsat Imagery. *Remote Sensing of Environment*. 106 (3), pp. 375–386.
18. Chen, X. L.; Zhao, H. M.; Li, P. X. and Yin, Z. Y. (2006). Remote Sensing Image based Analysis of the Relationship between Urban Heat Island and Land Use/Cover Changes. *Remote Sensing of Environment*. 104 (2), pp. 133–146.

19. Mutiibwa, D.; Strachan, S. and Albright, T. (2015). Land Surface Temperature and Surface Air Temperature in Complex Terrain. *IEEE Journal of Selected Topics in Applied Earth Observations and Remote Sensing*. DOI: 10.1109/JSTARS.2015.2468594.
20. Unger, J.; Gal., T.; Rakonczai, J.; Mucsi, L.; Szatmari, J.; Tobak, Z.; van Leeuwen, B. and Fiaala, K. (2009). Air Temperature versus Surface Temperature in Urban Environment. Paper presented at The Seventh International Conference on Urban Climate, 29 June- 3 July 2009, Yokohama, Japan.
21. Vadasz, V. (1994). On the Relationship between Surface Temperature, Air Temperature and Vegetation Index. *Advances in Space Research*. 14 (3), pp 3 (41) – 3 (44).
22. Ray, K.; Chincholikar, J. R. and Mohanty, M. (2013). Analysis of Extreme High Temperature Conditions over Gujarat. *Mausam*. 64 (3), pp 467-474.
23. Yu, X.; Guo, X. and Wu Z. (2014). Land Surface Temperature Retrieval from Landsat 8 TIRS—Comparison between Radiative Transfer Equation-Based Method, Split Window Algorithm and Single Channel Method. *Remote Sensing*. 6, 9829-9852; doi:10.3390/rs6109829.
24. U.S. Geological Survey (USGS), EarthExplorer. Available at: https://earthexplorer.usgs.gov/ (accessed in 2019).
25. Rajeshwari, A. and Mani, N. D. (2014). Estimation of Land Surface Temperature of Dindigul district using Landsat 8 data. *International Journal of Research in Engineering and Technology*. 3 (5), pp 122-126.
26. Walawender, J. P.; Hajto, M. J. and Iwaniuk, P. (2012). A new ArcGIS toolset for automated mapping of land surface temperature with the use of LANDSAT satellite data. Proc. IEEE IGARSS, 22–27 July 2012, Munich, Germany, 4371–4374, doi: 10.1109/IGARSS.2012.6350405.
27. National Aeronautics and Space Administration (NASA), "Landsat Data Continuity Mission," NASA, [Online]. Available: https://landsat.gsfc.nasa.gov/landsat-data-continuity-mussion/ .[Accessed: 2019].